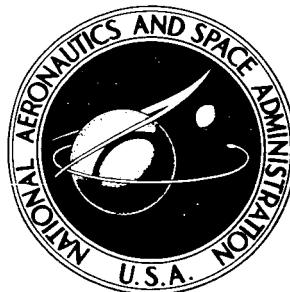


NASA TECHNICAL NOTE



NASA TN D-2605

NASA TN D-2605

FACILITY FORM 802

N65 14632
(ACCESSION NUMBER)

40
(PAGES)

(NASA CR OR TMX OR AD NUMBER)

(THRU)

1
(CODE)

30
(CATEGORY)

GPO PRICE \$ _____

OTS PRICE(S) \$ 2.00

Hard copy (HC) _____

Microfiche (MF) .50

MARS-NONSTOP ROUND-TRIP TRAJECTORIES

by Roger W. Luidens and Jay M. Kappraff

Lewis Research Center

Cleveland, Ohio

MARS NONSTOP ROUND-TRIP TRAJECTORIES

By Roger W. Luidens and Jay M. Kappraff

Lewis Research Center
Cleveland, Ohio

NATIONAL AERONAUTICS AND SPACE ADMINISTRATION

For sale by the Office of Technical Services, Department of Commerce,
Washington, D.C. 20230 -- Price \$2.00

MARS NONSTOP ROUND-TRIP TRAJECTORIES

by Roger W. Luidens and Jay M. Kappraff

Lewis Research Center

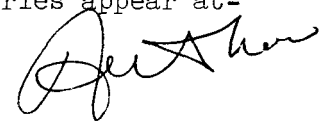
SUMMARY

14632

Manned and unmanned nonstop round trips may be precursors of the first manned landing on Mars. Lightweight vehicle systems and short mission durations are desirable. Three kinds of nonstop round-trip trajectories are analyzed. They are characterized by the method of turning that is used at Mars: (1) gravity only, (2) gravity supplemented by propulsion, and (3) gravity supplemented by aerodynamic forces. These trajectories are compared for the years 1970 to 1971 and 1979 to 1980 on the basis of total propulsive velocity increment, mission duration, Earth entry velocity, and view of Mars. For the missions using aerodynamic forces, the vehicle lift-drag ratio, g-load, and Mars entry velocity are presented.

Gravity turns occur only with mission durations near 360 or 550 days. The faster trips require the higher propulsive velocity increments. In comparison, the propulsion-gravity turn offers trip times as low as 400 days with little increase in total propulsive increment over that for the 550-day gravity turn. Of the three types of trajectories, the atmospheric turn trajectory offers the lowest total propulsive velocity increments. The minimum total propulsive velocity increment for atmospheric turn trajectories occurs for trips near 1 year in duration.

All three trajectory types yield at least an oblique view of the sunlit side of Mars. Also, the approach velocities at Earth are 65,000 feet per second or less. For the atmospheric turn trajectories, the Mars entry velocities are 47,000 feet per second or less, and the g-loads are below 7 Earth g's. Vehicles with a lift-drag ratio of 1.5 or larger are desirable. Missions are more difficult during the years of 1979 to 1980 than during 1970 to 1971 in terms of propulsive velocity increments and atmospheric entry velocities. The propulsion-gravity-turn and atmospheric-turn types of trajectories appear attractive for early nonstop round trips to Mars.



INTRODUCTION

Manned and unmanned nonstop round trips may be precursors of the first manned landing on Mars. The vehicle for such a trip will be launched from Earth and, without stopping, fly past Mars and return to Earth. In general, a vehicle placed on a trajectory to Mars will not return to Earth. In many

cases, however, an Earth return can be achieved if the trajectory is modified by one of the following means: (1) the gravity of Mars, (2) the gravity supplemented by propulsion, or (3) the gravity supplemented by aerodynamic forces. The trajectories resulting from the first kind of modification were analyzed in reference 1. This kind of trajectory occurs only with periods near those of orbits that are synchronous with the orbit of the Earth around the sun, that is, with periods near 1.0, 1.5, 2.0 years, and so forth, with the highest propulsion requirement occurring for the 1-year mission. This report contains an analysis of the characteristics of trajectories resulting from the second and third types of trajectory modification. Reduced propulsion requirements and a wider range of possible trip durations are goals to be sought with the increased freedom afforded by these modifications.

In this report, the preceding three kinds of nonstop round-trip trajectories are compared for the years 1970 to 1971 and 1979 to 1980 on the basis of the required total propulsive velocity increment, mission duration, Earth entry velocity, and view of Mars. The vehicle lift-drag ratio, g-load, and Mars entry velocity are presented for the trajectories using aerodynamic forces at Mars.

ANALYSIS

A typical nonstop round trip to Mars is shown in figure 1. In the present study, the mission starts in a circular orbit about Earth at 1.1 radii. A propulsive velocity increment is impulsively applied to send the space vehicle toward Mars. At Mars, the trajectory is modified in one of the aforementioned ways; at Earth return, atmospheric braking is used. As will be discussed in the section RESULTS AND DISCUSSION, the Earth approach velocities appear feasible for atmospheric braking. For the purpose of analysis, the overall trajectory is considered to be made up to interplanetary and planetary two-body segments that are matched at the sphere of influence of the planet.

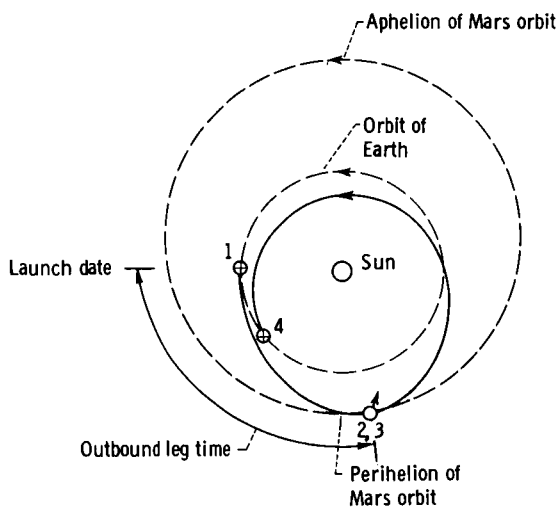


Figure 1. - Mars nonstop round-trip trajectory. Launch year, 1970 to 1971.

Interplanetary Trajectories

To determine the interplanetary trajectories, the motions and positions of Earth and Mars at specified times must be known. In the present analysis, the orbital motions of the planets as given by an ephemeris were approximated by mutually inclined ellipses (ref. 2) from which the planetary velocity vectors and positions were then calculated.

If the planetary motions are known, the characteristics of an Earth-Mars transfer trajectory are calculated as follows:

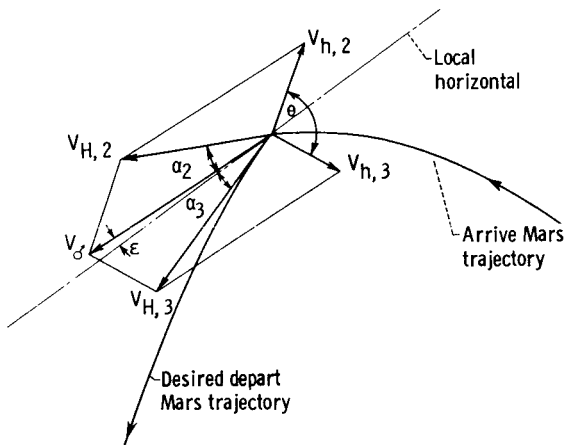


Figure 2. - Heliocentric and planetocentric velocity vectors at Mars sphere of influence.

(1) A launch date is specified. This defines the position and motion of the Earth when the space vehicle departs from Earth.

(2) An Earth-Mars transfer time is selected. This, together with the launch date, defines the position and motion of Mars at arrival of the space vehicle.

(3) The unique transfer trajectory, a conic section, which connects Earth and Mars in the specified outbound leg time, is found by using the procedure described in reference 2.

Similarly, a return transfer trajectory is defined by using the Mars departure date, which for nonstop missions is the arrival date, and by specifying the return trip time.

From the outbound and return transfer trajectories, the heliocentric path angles α_2 and α_3 (fig. 2) and the heliocentric velocities arriving at and departing from Mars $V_{H,2}$ and $V_{H,3}$ can be calculated. (The methods of ref. 2 were used to obtain trajectory data for the present analysis; however, some of the requisite interplanetary trajectory data are also tabulated in ref. 3.)

The previous procedure gives the arriving and leaving velocity vectors at Mars in coordinates centered on the Sun. In the vicinity of Mars, Mars rather than the Sun is the principal gravitating body. It is, therefore, appropriate and mathematically convenient to consider the trajectory near Mars in Mars-centered coordinates.

Mars-Centered Trajectories

A change in coordinates is made at the sphere of influence (ref. 2, p. 27). Inside the sphere of influence, Mars is assumed to be the only gravitating body; while outside this sphere, the Sun is considered the only gravitating body. The change is made by taking the difference between the vehicle heliocentric velocity vectors V_H and the planet velocity vector V_σ to give the planetocentric hyperbolic excess velocity vector V_h and the required turning angle at the sphere of influence θ (also illustrated in fig. 2). (All symbols are defined in appendix A.) The details of this calculation for mutually inclined orbits are also given in reference 2.

The arriving hyperbolic excess velocity vector may be considered to be located at any position on the arriving hemisphere at the sphere of influence. Similarly, the leaving hyperbolic excess velocity can be located at any position on the leaving hemisphere of the sphere of influence. There is, however, a unique location for these two velocity vectors on the sphere of influence

that yields a single plane containing Mars and the two velocity vectors. The Mars-centered trajectories are considered to be in this plane. (One of the functions of the interplanetary guidance and control system is to assure the attainment of the correct plane.)

A general trajectory within the sphere of influence and in the previously defined plane is shown in figure 3. Because of the planet gravity, the vehicle velocity increases along the hyperbolic approach segment from its value at the sphere of influence $V_{h,2}$ to $V_{p,2}$ at the trajectory periaapsis r_2 and changes direction by the angle δ_2 . Similarly, during departure, the vehicle velocity decreases along the hyperbolic segment from the value at the periaapsis $V_{p,3}$ to $V_{h,3}$ at the sphere of influence, and the change in direction by δ_3 . In general, the arrival velocity $V_{p,2}$ and the departure velocity, which will yield an Earth return $V_{p,3}$, are not equal in magnitude and are misaligned by the angle β at the periaapsis. Furthermore, because the radius and velocity vectors are normal at the periaapsis, the periaapsis radius vectors are also displaced by the angle β .

Several maneuvers that define the types of trajectories considered herein may be used to achieve the required matching of the arrival and departure velocities. First, combinations of Earth to Mars and Mars to Earth interplanetary trajectories may be sought that make $\beta = 0$ and $V_{p,2} = V_{p,3}$. Such trajectories are referred to as gravity turns. For this type of trajectory, the periaapsis radius r_p is a free variable and may be selected to yield the required matching. Second, the lift and drag forces generated in the planet atmosphere may be used to achieve the angular rotation β and to match the magnitude of $V_{p,2}$ to $V_{p,3}$. Such a maneuver is referred to as an atmospheric turn. The periaapsis radius is now restricted to be that of the sensible atmosphere. Finally, propulsion may be used for matching. As in the case of the gravity turn, the periaapsis radius is a free variable, and the propulsion may be applied anywhere along the trajectory within the sphere of influence. This type of maneuver is referred to as a propulsion-gravity turn. Each of these three kinds of maneuvers will be analyzed.

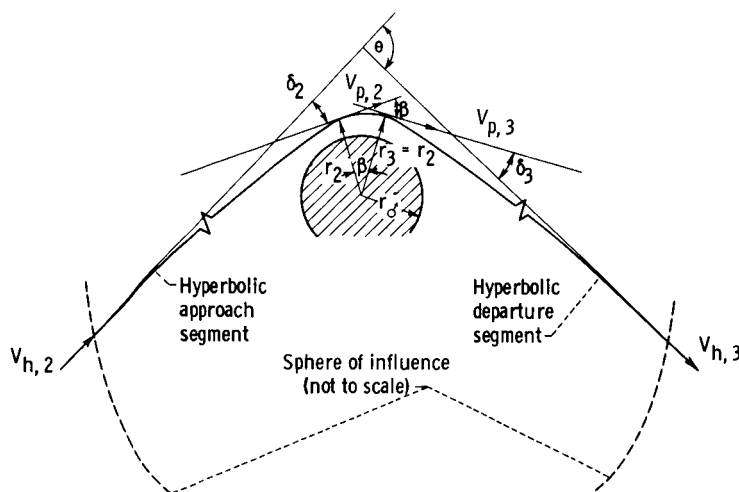


Figure 3. - General planetocentric trajectory in vicinity of Mars.

Turning Due to Gravity

Common to all of the trajectories within the sphere of influence is the turning due to the gravity of Mars along the approach and departure hyperbolas (fig. 3). These hyperbolic segments are completely defined by the hyperbolic excess velocity vector V_h and the trajectory periaapsis r_p . The flight path turning δ is (ref. 4)

$$\delta = \sin^{-1} \frac{1}{\frac{\bar{V}_p^2}{V_p^2} - 1} \quad (1)$$

The dimensionless periapsis velocity \bar{V}_p is the periapsis velocity divided by the circular velocity at the periapsis. It is related to the hyperbolic excess velocity through the conservation of energy by

$$\bar{V}_p = (\bar{V}_h^2 + 2)^{1/2} \quad (2)$$

where

$$\bar{V}_h \equiv \frac{V_h}{V_{c,p}} = \frac{V_h \sqrt{r_p}}{\sqrt{\mu_M}} \quad (3)$$

Gravity Turn Trajectories

These form the particular set of trajectories characterized by $\beta = 0$, for which $V_{p,2} = V_{p,3}$ and $\delta_2 = \delta_3$. Gravity turns exist when the gravity of Mars produces adequate or more than adequate turning ($\beta \leq 0$) for the closest allowable passage, 1.1 surface radii in the present calculations. If a close pass produces too much turning, then a higher periapsis will yield the desired value, as illustrated in figure 4. The required periapsis altitude may be found by equating the required turning as measured at the sphere of influence θ (see fig. 2) to the turning due to gravity

$$\theta = 2\delta_2 \quad (4)$$

From equations (1) to (4), the periapsis radius in Mars radii, $\bar{r} \equiv r/r_M$, is

$$\bar{r}_p = \frac{\frac{1}{\sin \frac{\theta}{2}} - 1}{\frac{V_{h,2}^2}{V_{c,\bar{r}=1.0}^2}} \quad (5)$$

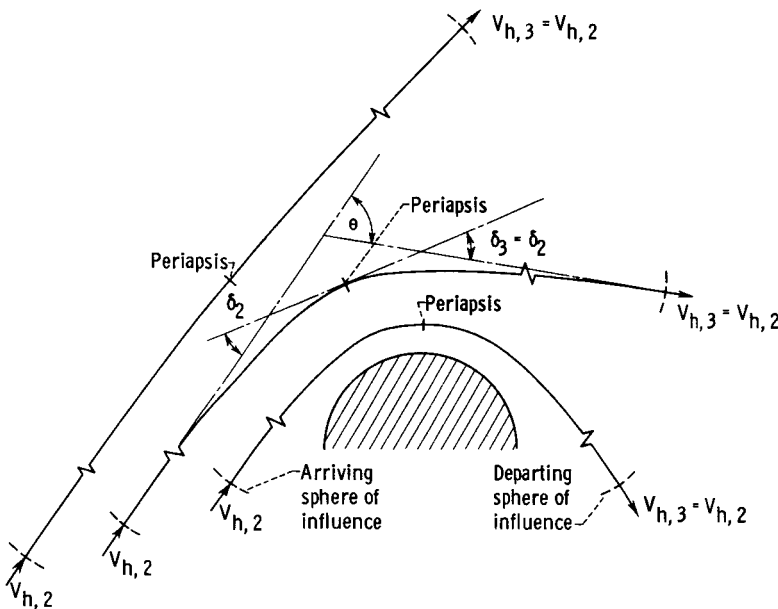


Figure 4. - Gravity turns at several periapsis altitudes.

Atmospheric Turn

Trajectories

A typical atmospheric turn maneuver is shown

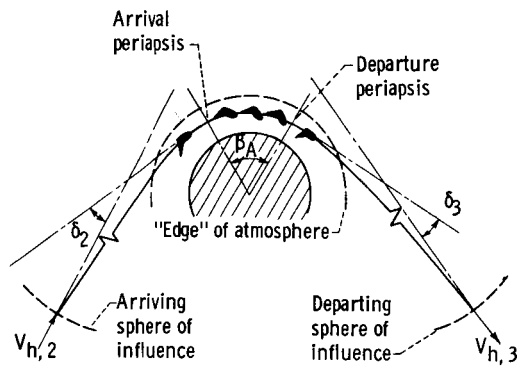


Figure 5. - Atmospheric turns.

in figure 5. It consists of three segments. The spacecraft approaches Mars along a hyperbolic segment, travels through the atmosphere along the atmospheric segment and departs Mars along a second hyperbolic segment.

For this case, the periapsis of the arrival and departure hyperbolas are taken as those periapses that would exist if Mars had no atmosphere. This is sometimes referred to as the vacuum periapsis. For com-

putational purposes, the vacuum periapsis has been taken at 1.05 Mars surface radii. The turning due to gravity during Mars arrival $\delta_{2,A}$ may then be found from equations (1) to (3) with

$$\bar{V}_{h,2,A} = \frac{V_{h,2}}{V_{c,\bar{r}=1.05}} \quad (6)$$

The turning along the departure hyperbola $\delta_{3,A}$ may be found similarly. The total turning due to gravity $\delta_{2,3,A}$ is then

$$\delta_{2,3,A} = \delta_{2,A} + \delta_{3,A} \quad (7)$$

A further assumption is that the vehicle velocity at the beginning and the end of the atmospheric flight is the velocity at the periapsis. This assumption simplifies the analysis of the atmospheric segment of the trajectory.

The flight in the Mars atmosphere must now provide a matching between the planet atmospheric approach and departure velocity vectors. This matching will be achieved by the aerodynamic lift and drag forces acting on a vehicle flying in the atmosphere at a constant lift-drag ratio (constant angle of attack). The lift provides the turning, while the drag produces a velocity decrease. The required periapsis turning angle β_A (see fig. 5) is

$$\beta_A = \theta - \delta_{2,3,A} \quad (8)$$

From a somewhat simplified model of the atmospheric flight, the vehicle lift-drag ratio necessary to achieve the required central turning angle and to match the planet approach and departure vectors is given by (ref. 5)

$$\frac{L}{D} = \frac{2\beta_A}{\ln \left(\frac{\bar{V}_{p,2}^2 - 1}{\bar{V}_{p,3}^2 - 1} \right)} \quad (9)$$

The corresponding maximum total load on the vehicle occurs at the initial

periapsis and in terms of Earth surface g 's is (ref. 5)

$$G_{\max} = \frac{g_0, \bar{r}=1.05}{g_{\oplus}} (\bar{V}_{p,2}^2 - 1) \left[1 + \frac{1}{\frac{L^2}{D}} \right]^{1/2} \quad (10)$$

(In practice, the altitude of the atmospheric flight must be chosen to yield the atmospheric density needed to generate the required aerodynamic forces. The required density is of the order of one-thousandth of the surface density of the Earth's atmosphere.) The preceding relations (eqs. (1) to (3) and (6) to (10)) permit analysis of the atmospheric turn trajectories.

Propulsion-Gravity Turn Trajectories

The required matching of the Mars arrival and departure velocity vectors can also be achieved by a combination of turning by gravity and propulsion. By definition of this particular case, propulsion is required and it is assumed that maximum use has been made of turning by gravity. Maximum gravity turning is achieved by a pass close to Mars. Therefore, in the present analysis, the periapsis of Mars passage is 1.1 Mars surface radii, which is assumed to be just high enough to avoid the atmosphere. Assuming the periapsis permits the calculation of the turning due to gravity in the manner described for the atmospheric turn trajectory. Consideration was given to applying propulsion at one of the following locations within the vicinity of Mars: (1) at the sphere of influence arriving at Mars, (2) at the sphere of influence leaving Mars, or (3) at the Mars periapsis.

Thrusting at sphere of influence. - The discussion here will be for the case of propulsion at the leaving sphere of influence (fig. 6(a)). It is applicable by analogy also to the case of propulsion at the arriving sphere of influence. The turning due to gravity from the arriving sphere of influence to the trajectory periapsis of 1.1 Mars radii δ_2 is similar to that given for the aerodynamic turn (eqs. (1) and (2)), for which equation (3) becomes

$$\bar{V}_{h,2,P} \equiv \frac{V_{h,2}}{V_{c, \bar{r}=1.1}} \quad (11)$$

The total turning from the arrival to the departure sphere of influence is $2\delta_{2,P}$. If θ (see fig. 2) is the total turning required, the turning required at the sphere of influence from the propulsive maneuver β_h is

$$\beta_h = \theta - 2\delta_{2,P} \quad (12)$$

The velocity at the leaving sphere of influence, prior to thrusting, is equal in magnitude to the velocity at the arriving sphere of influence $V_{h,2}$ (fig. 6(a)). The velocity required at the leaving sphere of influence to give the desired Earth return trajectory is $V_{h,3}$. By knowing $V_{h,2}$, $V_{h,3}$,

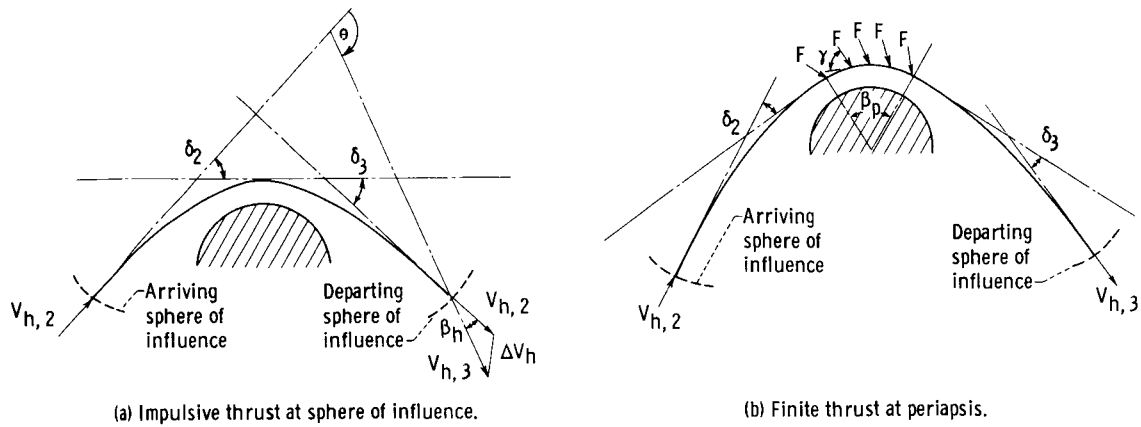


Figure 6. - Propulsion-gravity turns.

and β_h , the propulsive velocity increment required to match the inbound and outbound trajectories at Mars may be calculated from the law of cosines.

$$\Delta V_h = (V_{h,2}^2 + V_{h,3}^2 - 2V_{h,2}V_{h,3} \cos \beta_h)^{1/2} \quad (13)$$

For a given θ , $V_{h,3}$, and $V_{h,2}$ and for $V_{h,3} > V_{h,2}$, it can be shown (from eqs. (1), (2), (12), and (13)) that thrusting at the leaving sphere of influence will give a lower value of ΔV_h than thrusting at the arriving sphere of influence. This point is also discussed in the section Propulsion-Gravity Turns.

The proceeding calculation assumes an impulsive velocity change, which strictly speaking corresponds to an infinite g-load. To be effectively impulsive, however, the propulsive g-load need only be about equal to or larger than the local gravity field (of the order of $10^{-3} g_\oplus$.)

Finite thrusting at periapsis. - The third thrust location considered is at the trajectory periapsis. It is mathematically convenient to consider the case of continuous thrusting to maintain a constant altitude above the Mars surface, that is, at 1.1 Mars surface radii. This is illustrated in figure 6(b). For consistency with the other maneuvers, the continuous thrusting maneuver will be characterized by an equivalent ΔV , ΔV_p . For a constant specific impulse thruster, the ΔV_p is the time integral of the thrust to mass ratio

$$\Delta V_p \equiv \int_0^t \frac{F}{m} dt \quad (14)$$

The thrust is applied in a direction to maintain a constant altitude and thus is used in part to counter the centrifugal force not countered by gravity and in part to change the velocity dV_p/dt . The thrust is thus applied at an angle γ with respect to the flight path (or local horizontal)

$$F = \frac{m \frac{dV_p}{dt}}{\cos \gamma} \quad (15)$$

Combining equations (14) and (15) to eliminate dt and integrating, with a constant thrust angle γ assumed, give

$$\Delta V_p = \left(\frac{\bar{V}_{p,3} - \bar{V}_{p,2}}{\cos \gamma} \right) V_{c, \bar{r}=1.1} \quad (16)$$

The thrust angle, a constant, and the thrust magnitude, a variable, must be chosen both to yield a constant altitude and to produce the required velocity change. This problem is analogous to the atmospheric turn since flight in the atmosphere is equivalent to a constant maneuver altitude and a constant L/D is equivalent to a variable magnitude resultant force applied at a constant angle. In this analogy, the required thrust angle is the angle whose tangent is the lift-drag ratio. When the thrusting is used to increase the vehicle velocity at Mars, the required thrust angle is from equation (9)

$$\gamma = \tan^{-1} \frac{2\beta_p}{\ln \left(\frac{\bar{V}_{p,3}^2 - 1}{\bar{V}_{p,2}^2 - 1} \right)} \quad (17)$$

The maximum g-load occurs at the end of the powered maneuver and is equal to

$$G_{\max} = \frac{g_{\infty, \bar{r}=1.1}}{g_{\oplus}} \left(\bar{V}_{p,3}^2 - 1 \right) \left(1 + \frac{1}{\tan^2 \gamma} \right)^{1/2} \quad (18)$$

(see eq. (10)). The question of whether thrusting at the sphere of influence or at the periapsis yields the lower ΔV is discussed in the section Propulsion-Gravity Turns.

Propulsive Requirements to Leave Earth

The propulsive velocity increment required to reach Mars depends solely on the launch date and the outbound leg time. The unique transfer conic determined by these inputs fixes the hyperbolic excess velocity at Earth in a way similar to that in which the hyperbolic excess velocity was determined at Mars. The perigee velocity can then be calculated from equation (2) for a perigee radius of 1.1 Earth radii. The propulsive velocity increment required to leave Earth is then

$$\Delta V_1 = V_{p,1} - V_{c,\oplus} \quad (19)$$

Analysis of Trajectory Data

The preceding methods permit the calculation of the characteristics of a specified trajectory. There remain the problems of defining and finding favorable trajectories. The feasibility and desirability of nonstop round trips to Mars will be discussed in terms of the following criteria:

ΔV_T	total velocity increment to perform mission, that is, ΔV_1 for gravity and atmospheric turn trajectories, and $\Delta V_1 + \Delta V_h$ or $\Delta V_1 + \Delta V_p$ for propulsion-gravity turn trajectories
T_T	total trip duration
L/D	vehicle L/D required for atmospheric turn at Mars (pertinent only to atmospheric turn trajectory)
G_{\max}	maximum g-load during maneuver at Mars
$V_{p,4}$	approach velocity at Earth
$V_{p,2}$	approach velocity at Mars
r_p	periapsis of Mars passage

In general, low values of the aforementioned parameters are desirable. Because the initial weight in the Earth orbit is exponentially related to the propulsive ΔV , a low value of this parameter is especially important. A short mission duration is desirable for reliable operation and, for manned trips, to reduce life support weight and for psychological reasons. Vehicles with low lift-drag ratios are generally easier to design aerodynamically and have lower structural fractions than vehicles with high L/D . Low g-loads also tend to reduce the structural fractions. Also, for manned missions the g-loads must be within human tolerance and preferably near Earth surface gravity. The planet approach velocities are an indication of the degree of difficulty of the atmospheric entry and of the heat protection weight. Also, the accuracy required of the planet approach guidance system, the propulsive ΔV required for planet approach, and the observation time near the planet are related to the approach velocity. Again low values are preferable. The view of Mars is determined by the direction of approach to Mars and the altitude of the periapsis. In the present analysis, first priority has been given to finding trajectories requiring a low propulsive velocity increment.

The aforementioned criteria are determined from the outputs of the interplanetary trajectory calculations, which are

$V_{h,1}$ or ΔV_1	hyperbolic excess velocity at Earth departure, or propulsion velocity increment to leave Earth
$V_{h,2}$	hyperbolic excess velocity at Mars arrival
$V_{h,3}$	hyperbolic excess velocity at Mars departure

- $V_{h,4}$ hyperbolic excess velocity at Earth arrival
- α_2, α_3 heliocentric path angles at Mars arrival and departure, respectively, which together with the velocities at Mars determine the required turning angle θ at Mars sphere of influence

The trajectory outputs are in turn determined by the following inputs:

- JD_1 launch date
- T_O outbound leg time
- T_T total trip time

The launch years of 1970 to 1971 and 1979 to 1980 were chosen for study because they yield approximately the easiest and most difficult trips, respectively. A systematic survey was made of the remaining variables.

Recall from the previous discussion that the parameters affecting the maneuver required at Mars are the magnitude of the velocities arriving at and leaving Mars and the turning angle between these velocity vectors. Figures 7 to 9 show a typical set of data dealing with these parameters. Figure 7 is typical of the format used for these figures; this format is used again in the section Atmospheric Turns. The dependent variable, which in this figure is the velocity leaving Mars $V_{p,3}$, is presented as a function of total trip time for

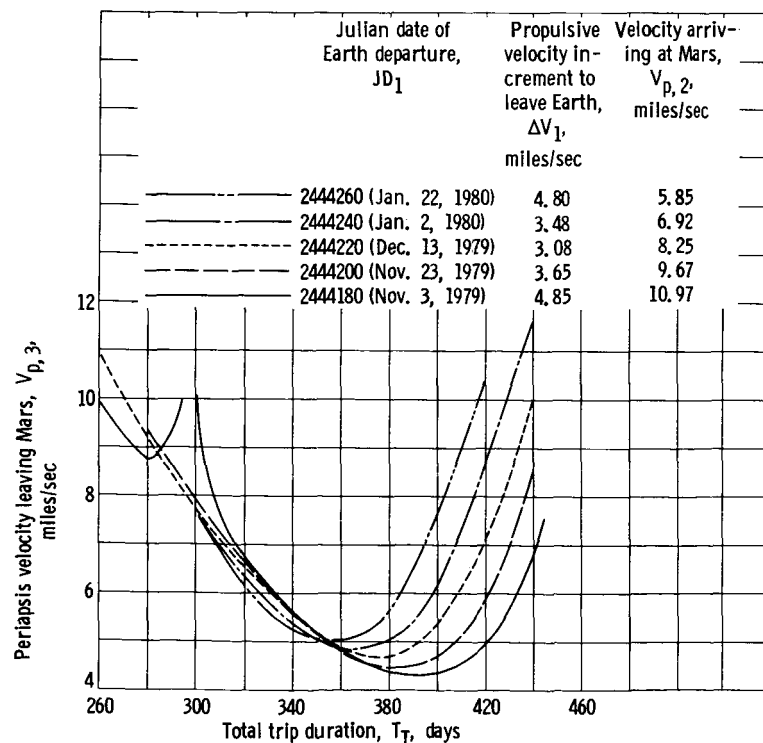


Figure 7. - Variation of velocity leaving Mars with total trip duration and date of Earth departure. Mars periapsis, 1.1 radii; launch year, 1979 to 1980; outbound leg time, 120 days.

a series of Julian dates for Earth departure. The curves apply for the 1979 to 1980 synodic period and for an outbound trip time of 120 days. For a given outbound trip time, the ΔV to leave Earth ΔV_1 and the velocity approaching the periapsis of Mars $V_{p,2}$ are functions only of the Julian date of Earth departure. The values of these parameters are listed in the figure. Figures 8 and 9 and later figures use the same abscissa and field parameters to present other dependent variables.

(The particular set of coordinates and field parameters selected for this group of figures was the most convenient and economical set for presentation

of the data resulting from the present method of calculation. The data in this form are also convenient for illustrating the factors affecting trip selection. The period 1979 to 1980 gave the less complex families of curves.)

Figure 7 shows that, for all Earth departure dates, a strong minimum in the velocity leaving Mars $V_{p,3}$ occurs at a total trip time in the vicinity of 350 to 400 days. (This minimum, for example, will have an important influence on the required L/D, as will be shown in the section Atmospheric Turns.) As may be seen from the values tabulated in the figure, the velocity arriving at Mars $V_{p,2}$ decreases for the later Earth departure dates. Also, ΔV_1 has a minimum for a Julian departure date of 2444220. (The anomalous increase in $V_{p,3}$ for $JD_1 = 2444180$ at a total trip time of about 300 days occurs in the present calculations when the transfer angle between Mars and Earth is near 180° and the transfer plane is significantly inclined to the ecliptic plane. It will also appear in subsequent figures. This anomaly can be avoided by using a midcourse plane change as explained in ref. 2.)

For the purposes of the subsequent discussion, it is convenient to form the parameter $V_{p,2} - V_{p,3}$ from the data of figure 7. The parameter is presented in figure 8. As would be expected, the shapes of the curves reflect the shape of the $V_{p,3}$ curves of figure 7. Positive, negative, and zero values of the parameter occur, and the value of the parameter decreases with later launch dates because $V_{p,2}$ decreases.

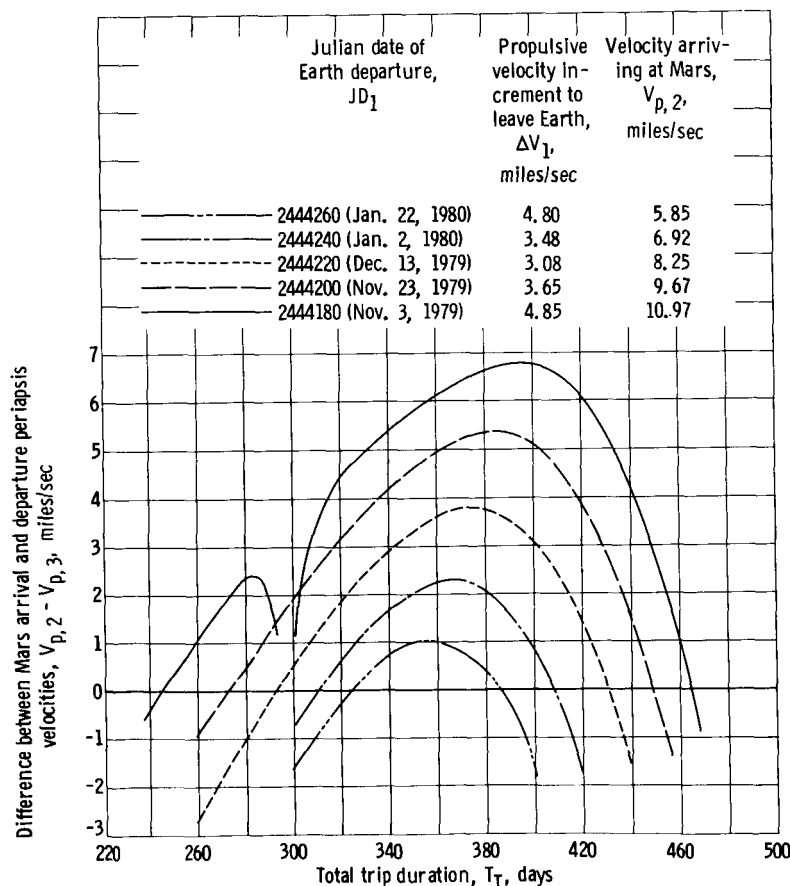


Figure 8. - Variation of difference between Mars arrival and departure periapsis velocities with total trip duration and date of Earth departure. Mars periapsis, 1.1 radii; launch year, 1979 to 1980; outbound leg time, 120 days.

Figure 9 presents the periapsis turning angle β (see fig. 3, p. 4) required at Mars for a periapsis of 1.1 radii. In the range of variables presented, the turning angles are all positive. The required turning angle decreases with increasing mission duration and for later launch dates.

The velocities of the spacecraft at Earth return are shown in figure 10. These velocities are generally below 12 miles per second for trip times of

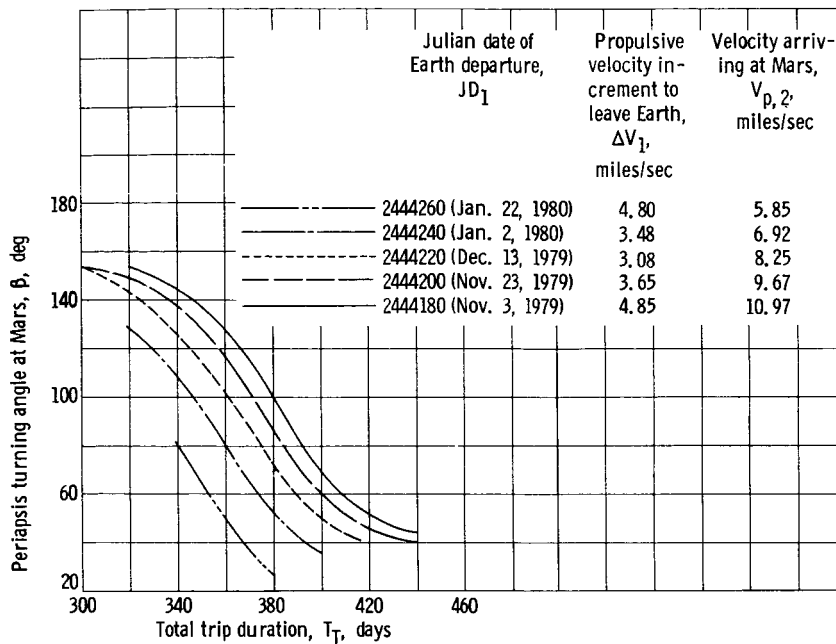


Figure 9. - Variation of turning angle required at Mars with total trip duration and date of Earth departure. Mars periapsis, 1.1 radii; launch year, 1979 to 1980; outbound trip time, 120 days.

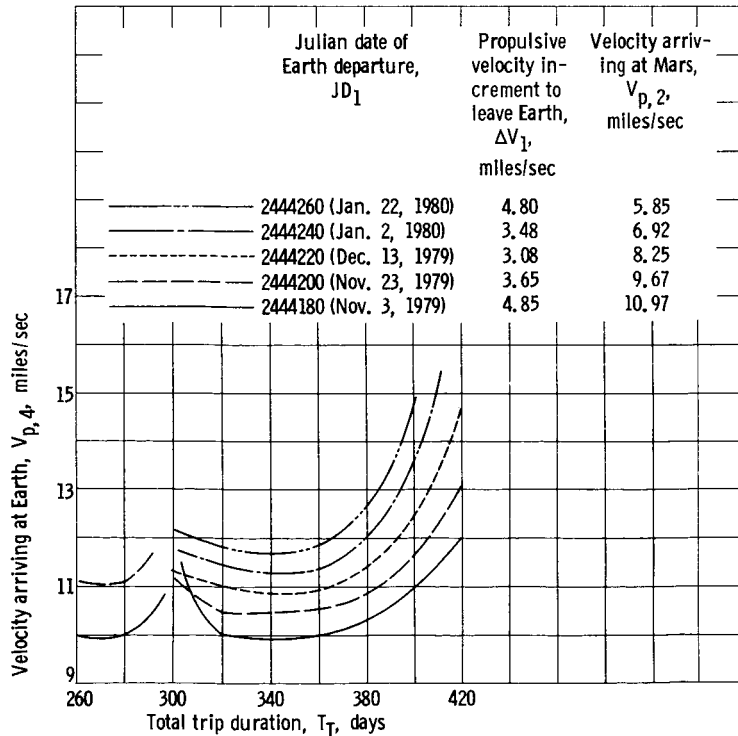


Figure 10. - Variation of Earth arrival velocity with total trip duration and date of Earth departure. Launch year, 1979 to 1980; outbound leg time, 120 days.

less than 360 days and increase for longer trip times. There is a decrease in the Earth return velocities for earlier launch dates.

Figures 7 to 10 were for an outbound leg time of 120 days. Similar sets of data exist for other outbound trip times. The three types of nonstop round trips will now be discussed within the context of such plots.

RESULTS AND DISCUSSION

Gravity Turns

Gravity turns occur when the Mars arrival and departure velocities are equal and the required sphere of influence turning angle θ is generated only by the Mars gravitational field. In

TABLE I. - CHARACTERISTICS FOR GRAVITY TURN TRAJECTORIES
WITH MINIMUM PROPULSIVE VELOCITY INCREMENT

Total trip, duration, T_T , days	Outbound leg time, T_O , days	Julian date of Earth departure, JD_1	Total propulsive velocity increment, ΔV_T , miles/sec	Velocity arriving at Earth, $V_{p,4}$, miles/sec
Launch year, 1970 to 1971				
360	80	2441160 (July 28, 1971)	4.3	9.7
500	210	2440980 (Jan. 29, 1971)	3.06	8.05
520	220	2440940 (Dec. 20, 1970)	3.37	7.75
540	250	2440900 (Nov. 10, 1970)	3.67	7.9
560	280	2440900 (Nov. 10, 1970)	3.99	8.1
Launch year, 1979 to 1980				
380	110	2444270 (Feb. 1, 1980)	5.9	13.7
540	260	2444055 (July 1, 1979)	4.9	11.70
560	280	2444015 (May 22, 1979)	6.24	10.95

terms of the parameters presented in figures 8 and 9, gravity turns require that the parameter $V_{p,2} - V_{p,3}$ (fig. 8) be zero and that the periapsis turning β , which exists for $r = 1.1$ radii (fig. 9), be negative, that is, that the gravity turning for such a close approach must provide more than adequate turning. The desired turning is then achieved by increasing the periapsis radius.

The data of figures 8 and 9 show that the required conditions are not quite satisfied for trips

with an outbound leg time of 120 days in 1979 to 1980. A systematic search over many outbound leg times does reveal gravity turn trajectories. Pertinent trajectory characteristics for gravity turn trajectories are given in table I. One such trip, for example, occurs for an outbound leg time of 110 days.

In figure 11, the propulsive ΔV for gravity turn trajectories (in this case, the ΔV leaving Earth orbit ΔV_1) is plotted against the mission duration in days. Because the Mars gravity can produce only a comparatively small perturbation on the interplanetary trajectory, gravity turns occur only in the vicinity of orbits that are synchronous with Earth's period about the Sun, neglecting the influence of Mars. In the range of trip times studied herein, synchronous orbits exist at 1.0 and 1.5 years. Figure 11 shows that gravity turns indeed occur in the vicinity of these times, as has also been found by

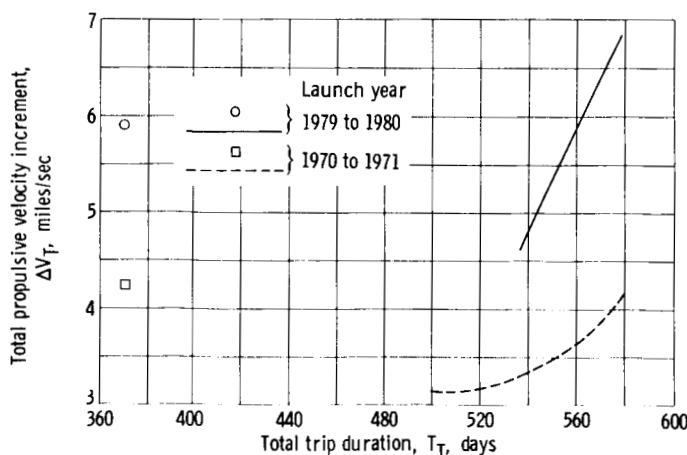


Figure 11. - Variation of minimum propulsive velocity increment with total trip duration for gravity turn trajectories.

others (e.g., refs. 1 and 6). The 1.0-year trip occurs only in a narrow region of trip times and requires a considerably higher ΔV than the 500- to 540-day trips, for example, 4.25 miles per second compared with 3.15 miles per second for 1970 to 1971. Also, trips in 1979 to 1980 require higher values of ΔV than those in 1970 to 1971, for example, 4.8 miles per second compared with 3.35 miles per second for a 540-day trip.

The 1.0-year trips have shorter outbound leg times, later launch dates (see table I), and

higher Earth return velocities than the 1.5-year trajectories. The Earth approach velocities for the 1.0- and 1.5-year trips are typically 9.7 and 8.0 miles per second respectively, in 1970 to 1971, and 13.7 and 11.0 miles per second, respectively, in 1979 to 1980.

The passage near Mars for trips in 1970 to 1971 of almost 1.5 years duration is described in more detail with the aid of figure 12. In this figure, the periapsis of Mars passage in Mars radii is plotted against the total trip duration in days. The synchronous orbit occurs at a trip time of 548 days and, by definition, corresponds to a passage at a great distance on either side of Mars, as illustrated, so the perturbation due to the gravity of Mars is negligible. For trip durations less than that of the synchronous orbit, the trajectories pass on the "dark" side of Mars and the radius of passage approaches the Mars surface as the trip time decreases. The lowest trip time, about 500 days, occurs for the assumed minimum permissible periapsis of 1.1 Mars radii.

The behavior of trajectories that are longer than 548 days is analogous to that of the shorter trips. The passage is now on the "Sun" side of Mars, and the periapsis of passage becomes less with increasing trip duration. The longest trip time is about 580 days, again corresponding to a passage at 1.1 Mars radii. The possible gravity turn trajectories in 1979 to 1980 behave similarly.

Propulsion-Gravity Turns

For these maneuvers, propulsion in addition to gravity is used to achieve the required matching between the arriving and departing velocity vectors at Mars. When propulsive turning is needed to satisfy the required total turning angle, the propulsion requirement is minimized if maximum use is made of the turning due to gravity. This is accomplished by passing as close as possible to the center of the gravitational field. In the present analysis, the periapsis of the Mars passage is 1.1 surface radii. In terms of parameters of figure 9 (p. 13), propulsion-gravity turns occur for positive β , that is, when turning, in addition to the maximum that gravity can provide, is needed. (Recall that when β is zero or negative gravity turns may be possible.)

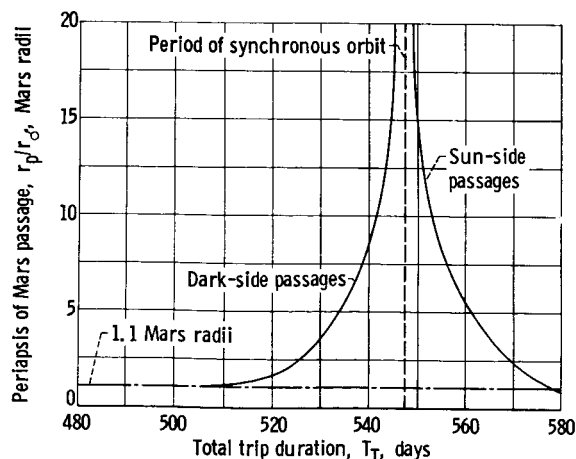


Figure 12. - Periapsis of Mars passage for gravity turn trajectories. Launch year, 1970 to 1971.

When propulsion is used, it can either increase or decrease the leaving velocity relative to the arriving velocity at Mars. Thus, the parameter $V_{p,2} - V_{p,3}$ of figure 8 (p. 12) can be either positive or negative. Three locations in the vicinity of Mars for thrusting were considered; they were (1) at the sphere of influence arriving at Mars, (2) at the sphere of influence leaving Mars, and (3) at the periapsis of Mars. If the only purpose of the

thrusting is to change the direction of the velocity vector, this is accomplished for the least ΔV when the velocity is the smallest. In the vicinity of Mars, this condition occurs at the sphere of influence. If the purpose of the thrust is also to increase the velocity a small amount, then, of the two sphere-of-influence positions, the leaving position is preferable because the turning due to the gravity of Mars is greater for the lower velocity within the sphere of influence. Conversely, if the thrusting is to decrease the velocity, of the two sphere-of-influence positions, the arriving position is preferable. Figure 8 (p. 12) presented the parameter $V_{p,2} - V_{p,3}$. By the foregoing discussion, if the parameter is positive, the arrival position on the Mars sphere of influence should be considered for thrusting; and conversely, if it is negative, the leaving position should be considered.

If the only purpose of the thrusting is to change the velocity magnitude, it can be shown that the best place to thrust is at the Mars periapsis and the thrust direction should be tangent to the velocity vector. This is based on the assumption that the resulting trajectory turning is acceptable. Figures 8 and 9 show examples (e.g., $JD_1 = 2444260$, $T_T = 400$ days) where the required periapsis turning in excess of that produced by gravity β is small (fig. 9) but $V_{p,2} - V_{p,3}$ (fig. 8) is substantial. If both a change in velocity magnitude and direction is to be made by thrusting at the periapsis, the maneuver is performed as described in the section ANALYSIS.

In general, there are many ways that thrust could be applied, single or multiple impulses or continuously. Only the case of a single thrusting period near Mars has been analyzed herein. For the single impulse case and for given arriving and leaving velocity vectors at the sphere of influence, there is a location on the trajectory within the sphere of influence that results in the least required ΔV_P to match the two trajectories. This problem was considered in reference 7. In appendix B, a comparison is made between the ΔV_P calculated with the present alternatives and the ΔV corresponding to the optimum location. The present approach yields values of ΔV_P that are too

large by no more than 0.06 mile per second or about 2 percent of ΔV_T .

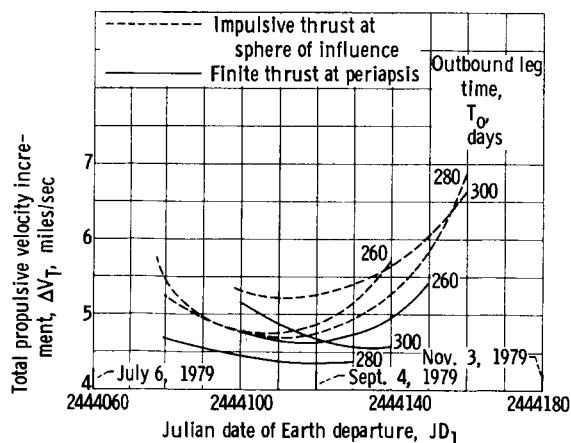


Figure 13. - Determination of best Earth departure date, outbound leg time, and thrusting location at Mars for propulsion-gravity turn trajectories. Launch year, 1979 to 1980; total trip duration, 520 days.

An example of how the trajectory data, which yield the ΔV_1 were combined with the ΔV_P for turning at Mars to find the trips that require the least total ΔV , is shown in figure 13. For a total trip time of 520 days, ΔV_T is plotted against the departure date for several outbound leg times and two thrusting locations at Mars. The arriving sphere-of-influence location was eliminated as a candidate position because a velocity increase was required. Of the two thrusting locations shown, the better is at the Mars periapsis

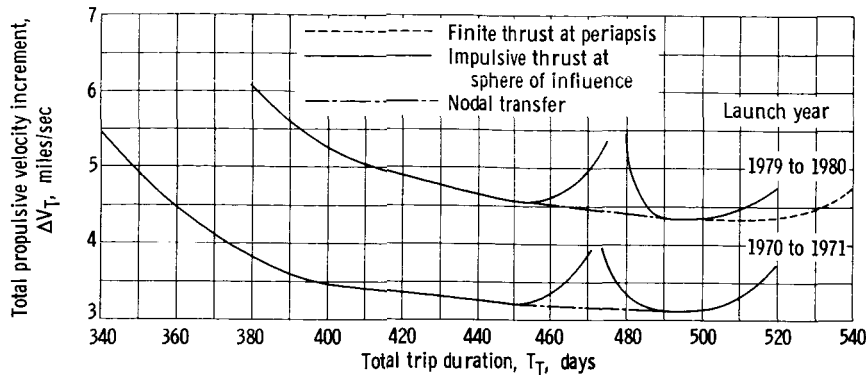


Figure 14. - Variation of minimum propulsive velocity increment with total trip duration for propulsion-gravity turn trajectories.

(solid lines in fig. 13). The curves also show a departure date, 2444120, and outbound trip time, 280 days, that approximately minimize ΔV_T .

The minimum propulsive ΔV from curves such as those of figure 13 were selected, and the results are plotted in figure 14 for both 1970 to 1971 and 1979 to 1980. For most of the total trip times, the best location for thrusting was at the sphere of influence leaving Mars (solid lines in fig. 14). Periapsis thrusting is better for the long trip times in 1979 to 1980 (dashed line in fig. 14).

Propulsion-gravity turn trips are possible over a wide range of trip times from less than 1.0 year to over 1.5 years. For trip times between 460 and 490 days the propulsive ΔV for the single-plane interplanetary trajectories (solid lines in fig. 14) increases abruptly. In this region, interplanetary trajectories using an optimum midcourse plane change (ref. 8) will yield performance approaching that given by the dash-dot line segments in figure 14.

The minimum ΔV_T occurs at about 500 days, and trips in 1970 to 1971 give significantly lower values of ΔV than those in 1979 to 1980, 3.14 compared with 4.3 miles per second. The ΔV_T , however, is only slightly greater than the minimum for trip times as low as 420 days. For still shorter trip times, the required ΔV_T rises significantly. The increase in ΔV_T for trip times longer than 500 days is due to the constraint placed on this set of calculations that the Mars periapsis be 1.1 surface radii. This results in too much gravity turning so that propulsive turning in the direction opposite to the gravity turning is required to achieve the required net turning angle at the sphere of influence θ . For 1970 to 1971, the gravity turns discussed previously yield lower values of ΔV for trip times between 500 and 520 days.

The outbound leg time, the Earth launch date, the propulsive values of ΔV , and the planet approach velocities are shown in table II for a series of minimum ΔV_T trajectories. In general, as the total trip time increases, the

TABLE II. - CHARACTERISTICS FOR PROPULSION-GRAVITY TURN TRAJECTORIES WITH MINIMUM PROPULSIVE VELOCITY INCREMENT

Total trip, duration, T_T , days	Outbound leg time, T_O , days	Julian date of Earth departure, JD_1	Total propulsive velocity increment, ΔV_T , miles/sec	Propulsive velocity increment at Mars, ΔV_p or ΔV_h , miles/sec	Velocity arriving at Earth, $V_{p,4}$, miles/sec	Ratio of Mars hyperbolic approach to circular velocity at periapsis, $\bar{V}_{h,2}$	Ratio of Mars hyperbolic departure to circular velocity at periapsis, $\bar{V}_{h,3}$	Ratio of Mars hyperbolic departure to approach velocity, $V_{h,3}/V_{h,2}$	Total required turning angle measured at Mars sphere of influence, θ , deg
Launch year, 1970 to 1971									
350	100	2441160 (July 28, 1971)	5.05	1.29	9.34	1.51	1.84	1.22	52.6
360	100	2441160 (July 28, 1971)	4.50	.79	9.56	1.51	1.84	1.22	40.9
380	100	2441140 (July 8, 1971)	3.85	.85	9.73	1.56	1.93	1.24	41.0
400	120	2441120 (June 18, 1971)	3.45	1.09	9.73	1.42	1.93	1.36	43.9
420	140	2441100 (June 3, 1971)	3.40	1.24	9.73	1.27	1.84	1.45	43.2
440	170	2441060 (Apr. 19, 1971)	3.35	1.01	9.44	1.42	1.79	1.26	43.7
460	180	2441040 (Mar. 30, 1971)	3.50	.914	9.20	1.65	1.79	1.09	47.4
480	200	2441000 (Feb. 18, 1971)	3.45	.662	8.71	1.65	1.65	1	47.6
Launch year, 1979 to 1980									
380	140	2444260 (Jan. 22, 1980)	6.19	1.64	12.51	1.84	2.03	1.16	48.5
400	160	2444240 (Jan. 2, 1980)	5.36	2.09	↓	1.75	↓	↓	58.2
420	180	2444220 (Dec. 13, 1979)	4.92	2.37	↓	1.75	↓	↓	63.2
440	200	2444220 (Dec. 13, 1979)	4.69	2.39	↓	1.75	↓	↓	73.2
460	220	2444180 (Nov. 3, 1979)	4.32	2.27	↓	1.60	↓	1.26	64.3
480	240	2444160 (Oct. 14, 1979)	6.49	2.49	↓	1.60	↓	1.26	60.3
500	260	2444140 (Sept. 24, 1979)	4.34	1.64	↓	1.39	↓	1.46	53.3
520	280	2444120 (Sept. 4, 1979)	4.35	1.38	↓	1.19	↓	1.71	44.0

outbound leg time increases and the launch date occurs earlier so that there is a broad spread of favorable launch dates corresponding to the range of trip times with low values of ΔV . The propulsive ΔV required at Mars ranges from about 17 to 53 percent of the total propulsive ΔV . The velocities at Earth approach are about 9.7 miles per second in 1970 to 1971 and 12.5 miles per second in 1979 to 1980. The last four columns of table II are discussed in appendix B.

For thrusting at the sphere of influence, the g-load required to approach the impulsive condition assumed is very low, for example, $10^{-3} g_\oplus$. For the finite thrusting at the Mars periapsis, the g-loads are generally less than $10 g_\oplus$'s.

Atmospheric Turns

For this type of trajectory, forces generated in the Mars atmosphere are used to match the arriving and leaving velocity vectors at Mars. There are two conditions for the existence of the type of aerodynamic turns considered here:

(1) The Mars departure velocity must be less than the Mars arrival velocity, or the parameter $V_{p,2} - V_{p,3}$ must be positive. This condition must hold because the drag of the vehicle in the atmosphere can only decelerate the vehicle.

(2) The turning angle in the atmosphere must be in the same direction as

the turning angle due to gravity during Mars arrival and departure. This is the case illustrated in figure 5 (p. 6) and is referred to as positive turning $\beta_A > 0$. (If the vehicle lift were applied in the opposite direction from that shown, that is, away from the planet, so-called negative turning could be generated. Negative turns, however, have not been considered here.)

Figure 8 (p. 12) presents the parameter $V_{p,2} - V_{p,3}$, which must be positive to satisfy condition 1. There are extensive regions of positive values in the vicinity of total trip times of 1.0 year. There are regions of total trip times longer and shorter than 1.0 year where, for a given launch date, atmospheric turns are not possible because $V_{p,2} - V_{p,3}$ is negative.

The required atmospheric turning angles are presented in figure 9 (p. 13). In the range of variables considered in this figure, they are all positive, and thus condition 2 is satisfied.

The data of figures 7 and 9 may be used in equations (9) and (10) to yield the required aerodynamic vehicle lift-drag ratio and the maximum g-load. These parameters are presented in figures 15 and 16. Low values of L/D (fig. 15)

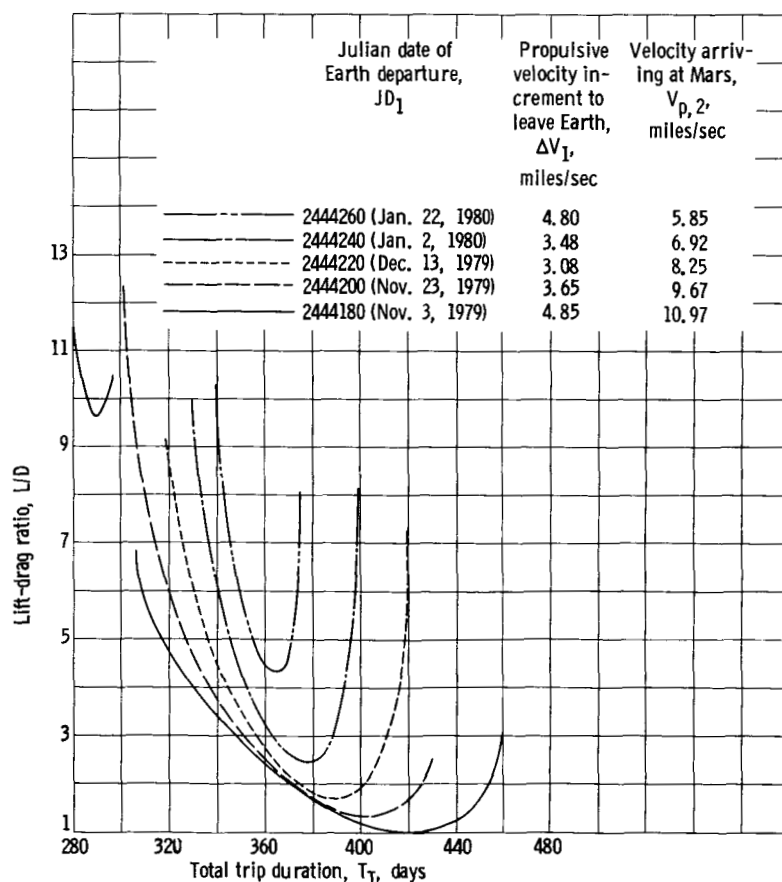


Figure 15. - Variation of lift-drag ratio with total trip duration and date of Earth departure. Launch year, 1979 to 1980; outbound leg time, 120 days.

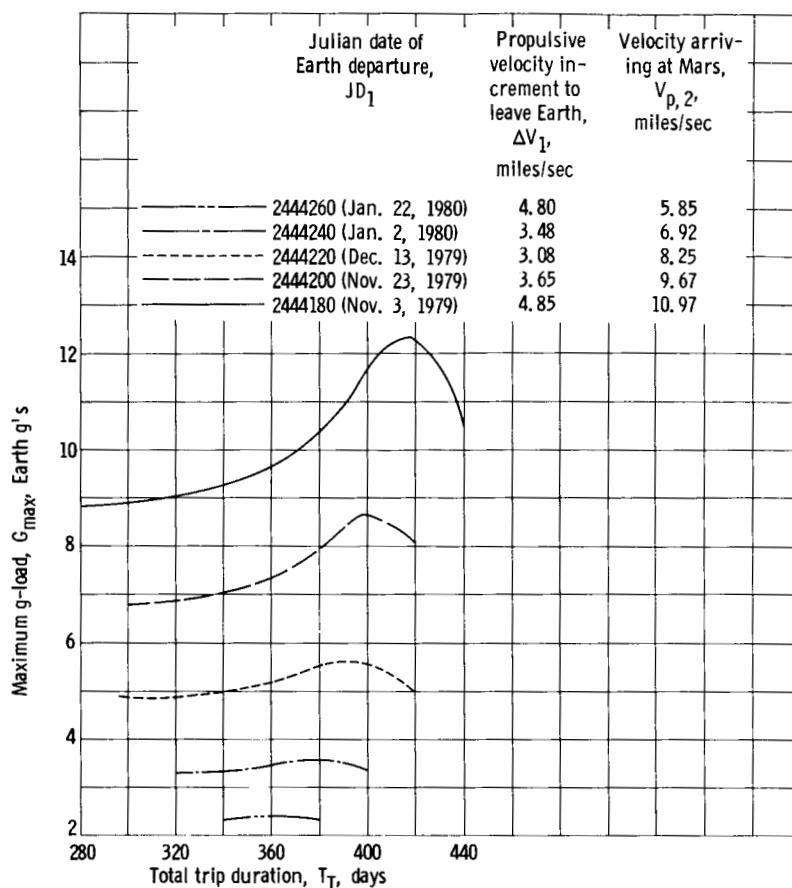


Figure 16. - Variation of maximum g-load in atmospheric turn at Mars with total trip duration and date of Earth departure. Launch year, 1979 to 1980; outbound leg time, 120 days.

occur for trip times of 380 to 440 days and for early launch dates (e.g., 2444180). This is where the required turning in the atmosphere β is small (see fig. 9) and when the velocity difference $V_{p,2} - V_{p,3}$ is large (see fig. 8). Physically, to produce a large velocity decrease in a small atmospheric turning angle β_A requires a large drag and, hence, low values of the lift-drag ratio. Similarly, when $V_{p,2} - V_{p,3}$ approaches zero, little or no drag is permissible, and the required lift to drag ratios approach infinity. This is the situation at the longer and shorter trip times.

The maximum g-load, presented in figure 16, is the initial g-load on a given atmospheric trajectory segment and depends on the velocity arriving Mars $V_{p,2}$ and the vehicle L/D (see eq. (10)). The most obvious feature of this figure is the increase in g-load with earlier launch dates. The early launch dates have the higher velocities arriving at Mars as noted in the key of the figure. The g-loads are all below 13 Earth g's for the cases that are presented.

The preceding discussion dealt with an outbound leg time of 120 days in 1979 to 1980. Figures 17 to 20 present vehicle lift-drag ratios against total

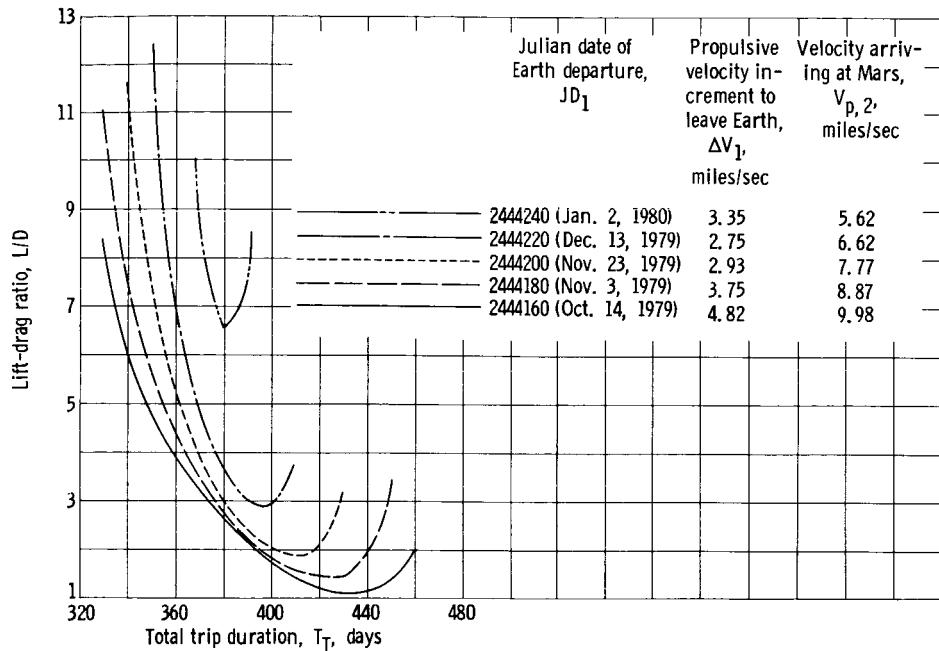


Figure 17. - Variation of lift-drag ratio with total trip duration and date of Earth departure. Launch year, 1979 to 1980; outbound leg time, 140 days.

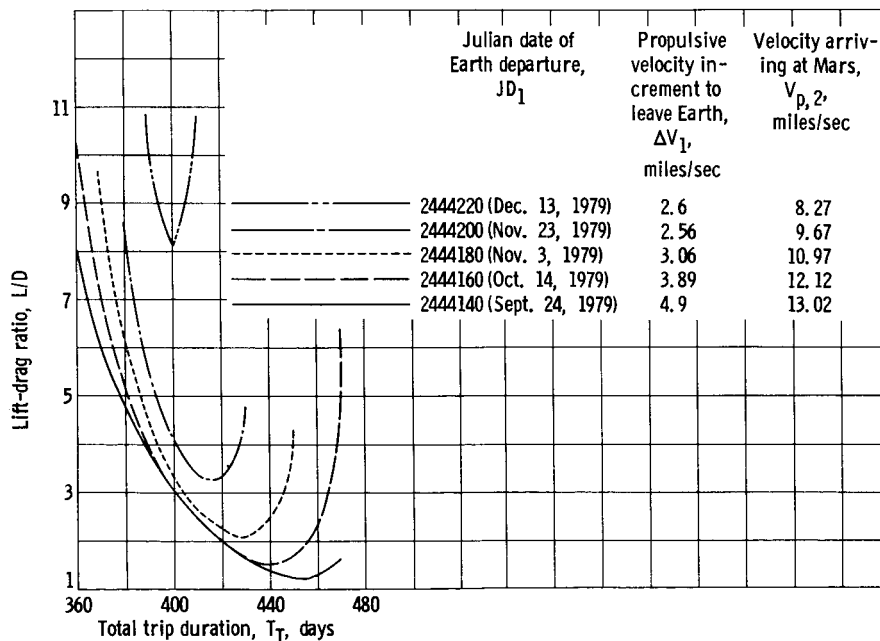


Figure 18. - Variation of lift-drag ratio with total trip duration and date of Earth departure. Launch year, 1979 to 1980; outbound leg time, 160 days.

trip time with parametric variations of launch date and corresponding variations in ΔV to leave Earth and velocity arriving at Mars (tabulated on the curves) for outbound leg times of 140, 160, 180, and 200 days. The general shapes of the curves are similar to those for 120-day time out. The g-load for these trips are generally less than 10 g_{\oplus} 's. The trajectory data $V_{p,3}$, $V_{p,4}$,

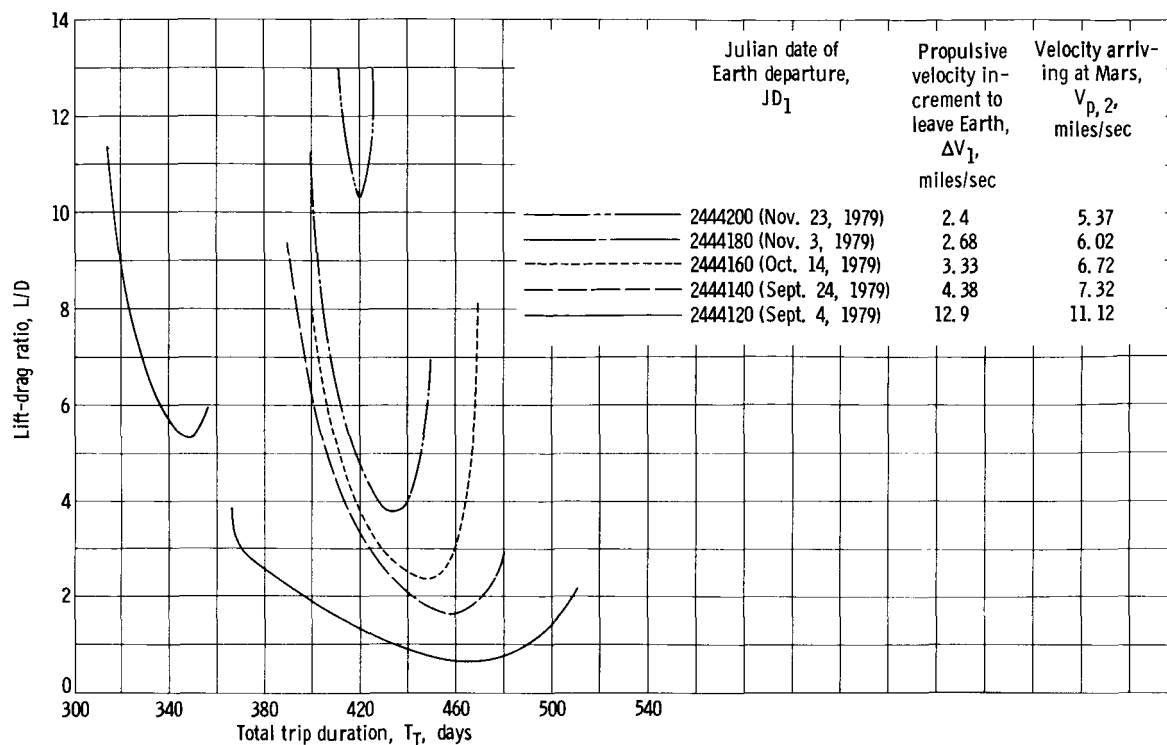


Figure 19. - Variation of lift-drag ratio with total trip duration and date of Earth departure. Launch year, 1979 to 1980; outbound leg time, 180 days.

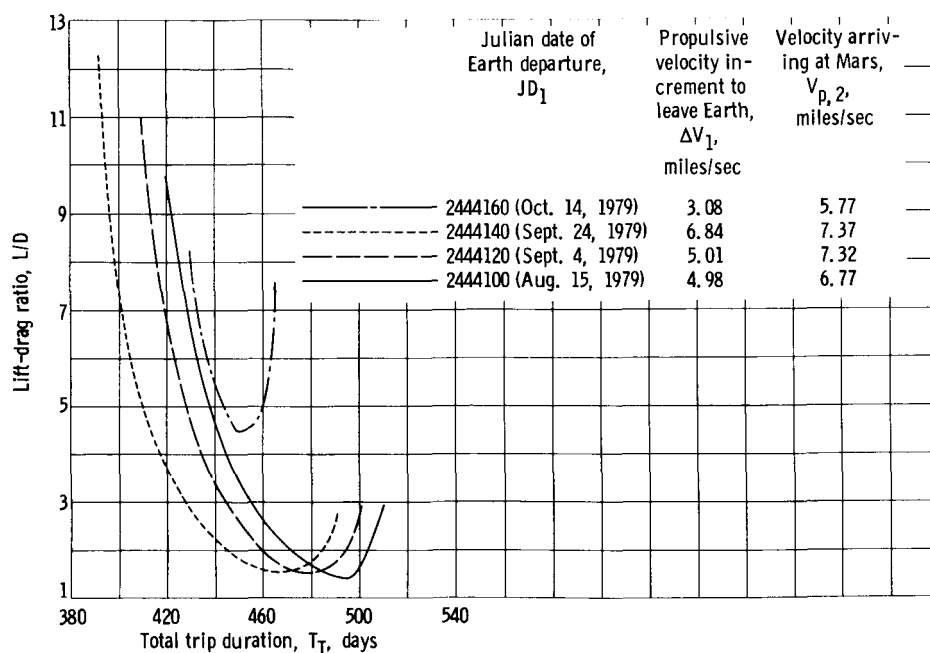


Figure 20. - Variation of lift-drag ratio with total trip duration and date of Earth departure. Launch year, 1979 to 1980; outbound leg time, 200 days.

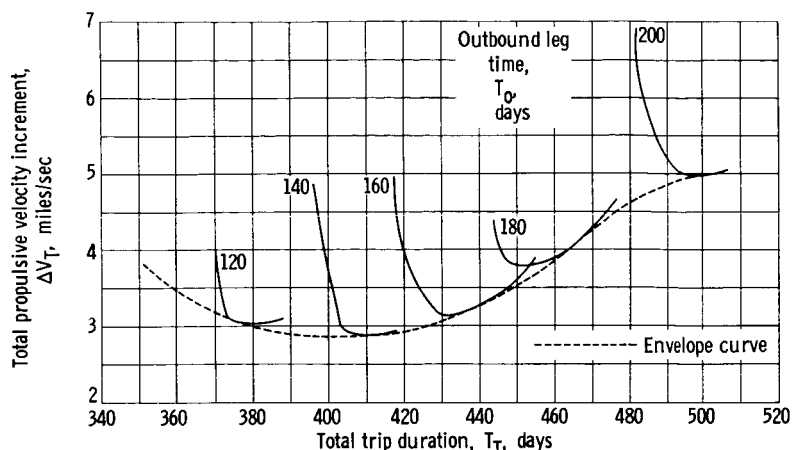


Figure 21. - Determination of minimum propulsive velocity increment as a function of total trip duration for atmospheric turn trajectories. Launch year, 1979 to 1980; lift-drag ratio, 2.

and β_A were also obtained but are not presented.

There are several approaches that could be taken to further analyze these data. The present approach is essentially a search for minimum ΔV missions. The data of figures 15 and 17 to 20 are cross-plotted in figure 21 for a constant value of lift-drag ratio $L/D = 2.0$. For each outbound leg time, there is a curve of ΔV against trip time. The curve for each time out

exhibits a minimum as would be expected from the previous data. An envelope of these curves yields the lowest ΔV for a given trip time.

Corresponding to minimum ΔV envelope curves there are curves of maximum g-loads and of the velocities at arrival at Mars and Earth. These data constitute the final results for atmospheric turn trajectories.

Minimum propulsive ΔV envelope curves as a function of total trip time for several values of lift-drag ratio are presented in figures 22 and 23 for launch years of 1970 to 1971 and 1979 to 1980, respectively. The corresponding values of G_{max} and the Mars and Earth arrival velocities are presented in figures 24 to 29, and the Earth departure dates and outbound leg times are given in table III.

Figure 22 for 1970 to 1971 shows that atmospheric turn trajectories are possible over a wide range of trip durations, 260 to 500 days. The minimum

TABLE III. - CHARACTERISTICS FOR ATMOSPHERIC TURN TRAJECTORIES WITH MINIMUM PROPULSIVE VELOCITY INCREMENT

Outbound leg time, T_O , days	Lift-drag ratio							
	1.0		1.5		2.0		4.0	
	Julian date of Earth departure, JD_1	Total trip duration, T_T , days	Julian date of Earth departure, JD_1	Total trip duration, T_T , days	Julian date of Earth departure, JD_1	Total trip duration, T_T , days	Julian date of Earth departure, JD_1	Total trip duration, T_T , days
Launch year, 1970 to 1971								
80	2441060 (Apr. 19, 1971)	340	---	---	---	---	---	---
80	2441080 (May 9, 1971)	370	2441100 (May 29, 1971)	350	2441100 (May 29, 1971)	325	2441105 (June 3, 1971)	280
100	2441055 (Apr. 14, 1971)	390	2441080 (May 9, 1971)	380	2441090 (May 19, 1971)	380	2441100 (May 29, 1971)	340
120	---	---	2441055 (Apr. 14, 1971)	400	2441065 (Apr. 24, 1971)	400	2441085 (May 14, 1971)	400
140	2441015 (Mar. 5, 1971)	430	2441030 (Mar. 20, 1971)	420	2441040 (Mar. 30, 1971)	430	2441055 (Apr. 14, 1971)	440
160	---	---	2441010 (Feb. 28, 1971)	450	2441020 (Mar. 10, 1971)	450	2441010 (Feb. 28, 1971)	470
Launch year, 1979 to 1980								
100	2444180 (Nov. 3, 1979)	395	2444220 (Dec. 13, 1979)	362	2444230 (Dec. 23, 1979)	350	---	---
110	2444190 (Nov. 13, 1979)	405	2444220 (Dec. 13, 1979)	382	2444230 (Dec. 23, 1979)	363	---	---
120	2444180 (Nov. 3, 1979)	420	2444210 (Dec. 3, 1979)	395	2444220 (Dec. 13, 1979)	375	2444220 (Dec. 13, 1979)	345
140	2444150 (Oct. 4, 1979)	440	2444180 (Nov. 3, 1979)	425	2444200 (Nov. 23, 1979)	413	2444220 (Dec. 13, 1979)	377
160	2444100 (Aug. 15, 1979)	465	2444160 (Oct. 14, 1979)	443	2444180 (Nov. 3, 1979)	430	2444200 (Nov. 23, 1979)	401
180	---	---	---	---	2444140 (Sept. 24, 1979)	472	2444180 (Nov. 3, 1979)	435

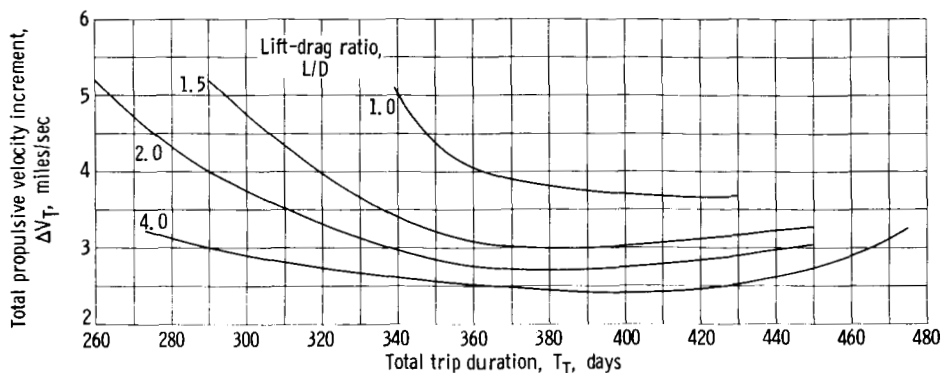


Figure 22. - Variation of minimum propulsive velocity increment with total trip duration and lift-drag ratio. Launch year, 1970 to 1971.

values of ΔV occur for trips of about 380 to 420 days duration. For an L/D of 1.5 or greater the values of ΔV increase slowly for trips of duration less than that for minimum ΔV . The lowest ΔV (2.42 miles/sec) occurs for a 400-day trip for a vehicle with an $L/D = 4.0$. The minimum values of ΔV increase as the available vehicle lift-drag ratio decreases. For instance at 400 days mission duration, the ΔV increases to 3.0 miles per second for $L/D = 1.5$ and to 3.5 miles per second for $L/D = 1.0$.

Figure 23 for 1979 to 1980 shows trends similar to figure 22. For a given L/D and trip time, the values of ΔV are slightly higher in 1979 to 1980 than in 1970 to 1971. Also, the minimum ΔV region is more restricted; for example, missions with an $L/D = 4$ vehicle can be made for a ΔV of less than 3 miles per second over a range of trip times from 290 to 460 days in 1970 to 1971. The comparable range of trip times in 1979 to 1980 is 355 to 450 days.

There is also a region of low L/D trips near the gravity turn trajectories in terms of trip time and ΔV_T . These were not considered to be of primary interest and are not presented.

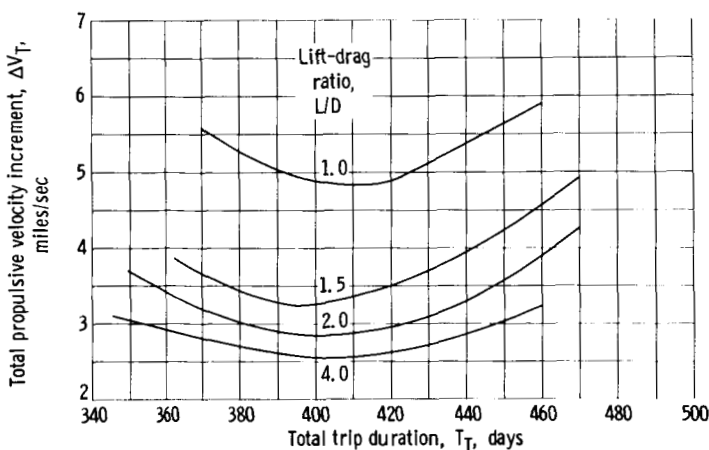


Figure 23. - Variation of minimum propulsive velocity increment with total trip duration and lift-drag ratio. Launch year, 1979 to 1980.

An important question at this point is what vehicle lift-drag ratios are feasible. Reference 9 (fig. 13) indicates that lift-drag ratios up to about 3.4 are aerodynamically feasible at Mach 20 in air for flat-top conical wing body combinations. These configurations have sharp or pointed leading edges and in light of present knowledge may not be feasible from a heat protection point of view. Reference 10 (figs. 12 and 13) indicates that $L/D = 2.0$ is possible with a

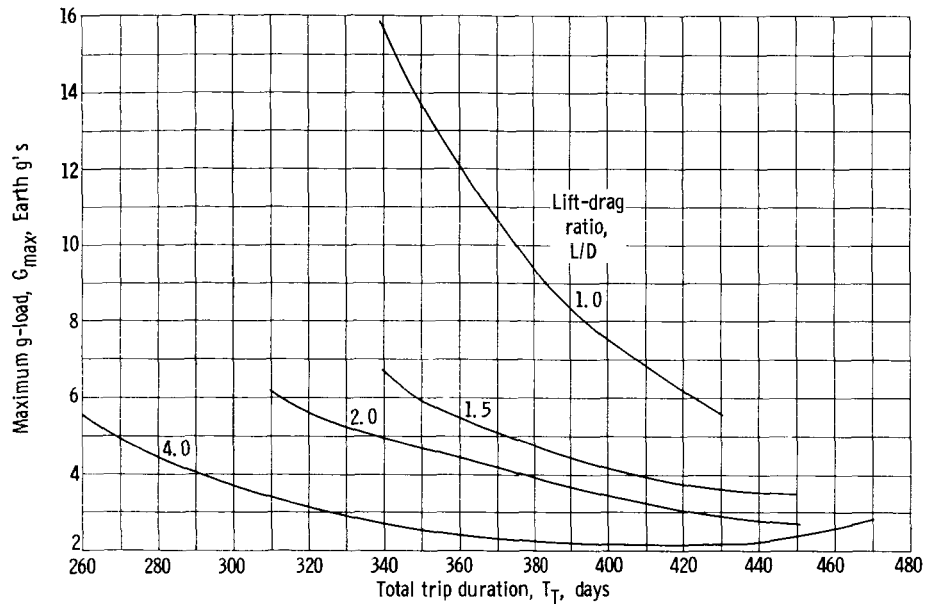


Figure 24. - Variation of maximum g-load in atmospheric turn at Mars with total trip duration and lift-drag ratio for trajectories with minimum propulsive velocity increment. Launch year, 1970 to 1971.

flat-top half cone with a half-cone angle of about 17° . Such a configuration is probably amenable to heat protection. Thus vehicles with lift-drag ratios of 2.0 or less may be in the feasible range. The ΔV advantage for vehicles with an L/D greater than 2.0 is small.

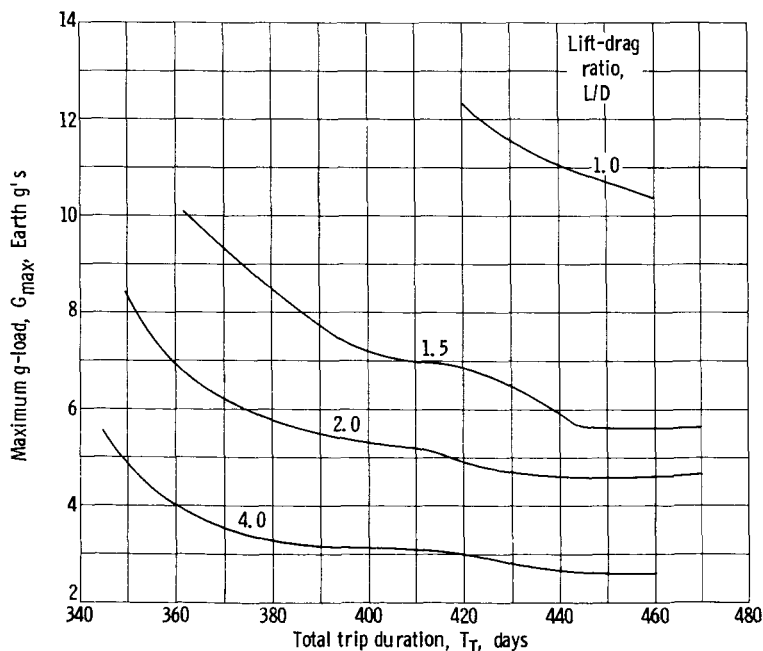


Figure 25. - Variation of maximum g-load in atmospheric turn at Mars with total trip duration and lift-drag ratio for trajectories with minimum propulsive velocity increment. Launch year, 1979 to 1980.

The maximum g-loads for the atmospheric turn at Mars are shown in figures 24 and 25. In general, the curves show the g-load decreases with increasing lift-drag ratio and increasing trip time. The human tolerance to g's is about 10 to 12 Earth g's for short periods of time. The g-loads at Mars exceed this limit only for $L/D < 1$ and trip times less than 480 days in 1979 to 1980. In the range of trip times for low ΔV , 400 to 420 days, and for vehicle $L/D \geq 1.5$, the g-loads are less than 4 Earth g's in 1970 to 1971. The g-loads are higher in 1979 to 1980 (fig. 25) but are less than 7 Earth g's for the previously mentioned conditions.

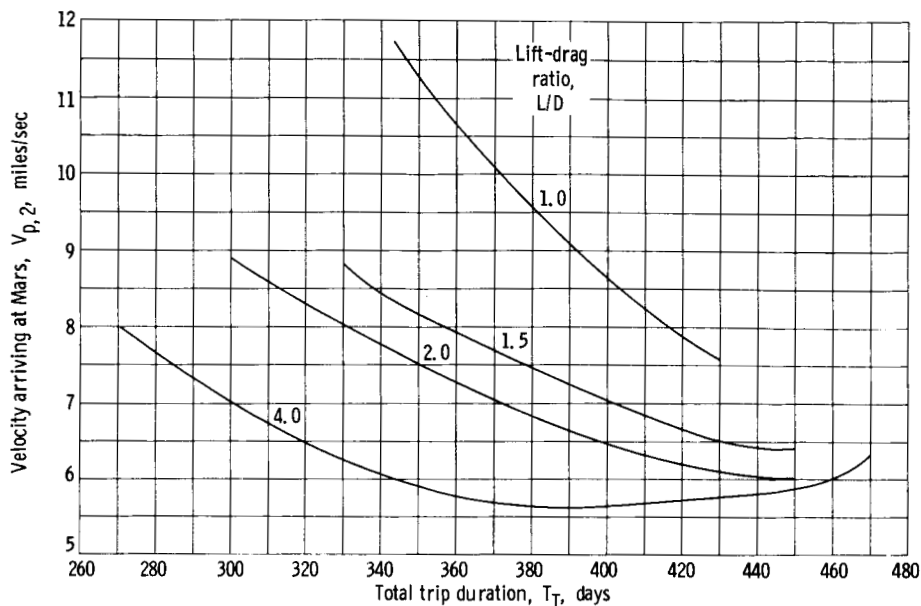


Figure 26. - Variation of velocity arriving at Mars with total trip duration and lift-drag ratio for atmospheric turn trajectories with minimum propulsive velocity increment. Launch year, 1970 to 1971.

In general, the g-loads are within the acceptable range.

The Mars atmospheric entry velocities are shown in figures 26 and 27. As was mentioned earlier, they show the same trends as the g-loads, that is, the entry velocities decrease with increasing L/D and increasing trip time. For trip times longer than 400 days and vehicle L/D greater than 1.5, the velocity arriving Mars for 1970 to 1971 is less than 7 miles per second (Earth parabolic velocity or 37,000 ft/sec). In 1979 to 1980, the entry velocities are higher; they are less than 9 miles per second for the aforementioned conditions.

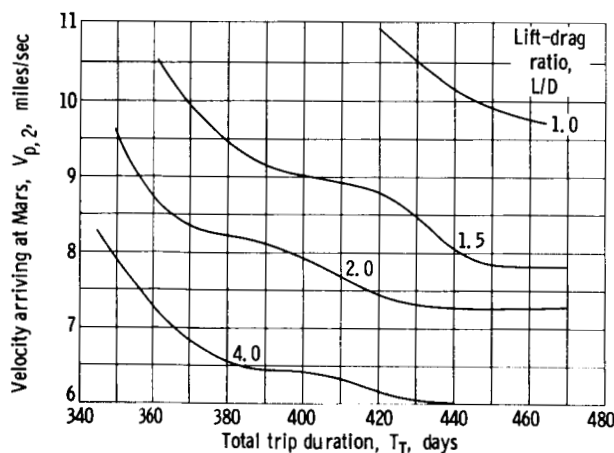


Figure 27. - Variation of velocity arriving at Mars with total trip duration and lift-drag ratio for atmospheric turn trajectories with minimum propulsive velocity increment. Launch year, 1979 to 1980.

The Earth approach velocities are given in figures 28 and 29. These values show only a small variation with trip duration and lift-drag ratio. In 1970 to 1971, the approach velocities are about 9 miles per second or less than twice the circular velocity of Earth. In 1979 to 1980, the approach velocities are about 12 miles per second.

A survey of the atmospheric entry problems at Mars and Earth is given in reference 11. From a heat protection point of view, atmospheric entries up to 13.4 miles per second appear possible for an $L/D = 0.5$ vehicle (ref. 11, fig. 26). The convective heating at Earth and Mars

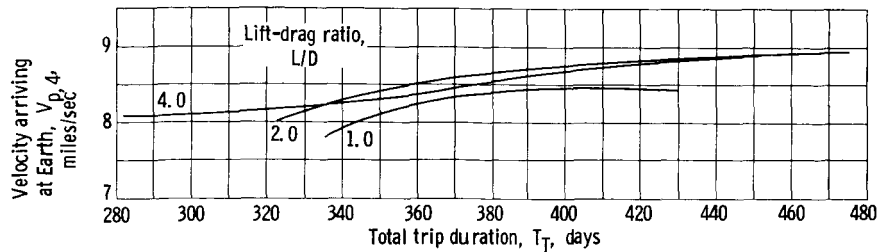


Figure 28. - Variation of velocity arriving at Earth with total trip duration and lift-drag ratio for atmospheric turn trajectories with the minimum propulsive velocity increment. Launch year, 1970 to 1971.

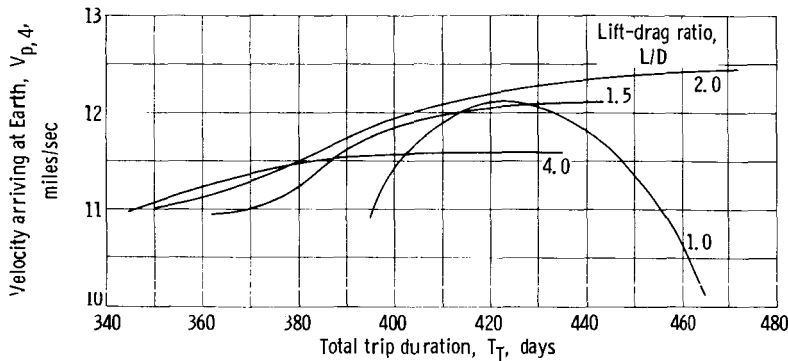


Figure 29. - Variation of velocity arriving at Earth with total trip duration and lift-drag ratio for atmospheric turn trajectories with the minimum propulsive velocity increment. Launch year, 1979 to 1980.

tends to be similar because of the large fraction of nitrogen in both atmospheres. Because of the combination of carbon dioxide and nitrogen in the Mars atmosphere, the hot gas radiative heating, in contrast, can pose a more difficult problem at Mars than at Earth. If the 17° half-angle cone vehicle previously mentioned is assumed, the radiative heating is small for either

an Earth or Mars entry (ref. 11, fig. 12). In general, the low surface angles associated with configurations of $L/D = 1.5$ or greater will result in low radiative heat inputs for either Earth or Mars. The Earth and Mars atmospheric entry velocities thus appear to be within the range of feasibility.

High lift to drag ratios (i.e., $L/D \geq 1.5$) are of greater importance to the atmospheric turn mission than most previously considered applications of atmospheric forces. For instance, an Earth entry at twice circular can reasonably be accomplished with an $L/D = 1.0$ vehicle. Hence there has been little detailed analysis and experimentation on the heat protection of high L/D vehicles at the velocities applicable to an atmospheric turn at Mars. This is an area for future effort.

Final evaluation of the atmospheric turn depends also on weight estimations of the heat protection systems, atmospheric entry corridors, guidance capabilities, and an overall mission analysis. These evaluations are beyond the scope of this study.

Summarizing, trajectory analysis indicates that, for the atmospheric turn type of trajectory, vehicle lift-drag ratios of 1.5 or greater are desirable. Lift-drag ratios of 1.5 to 2.0 appear aerodynamically feasible. For such lift-drag ratios, the g-loads and atmospheric entry velocities at Mars and Earth are within the range of feasibility. The requirements in 1970 to 1971 are less difficult than those in 1979 to 1980. The attractive feature of the atmo-

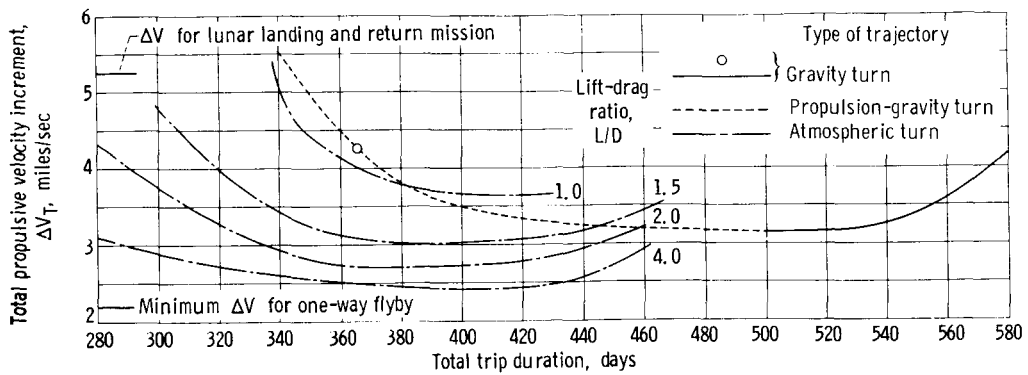


Figure 30. - Mars nonstop round trips, Launch year, 1970 to 1971.

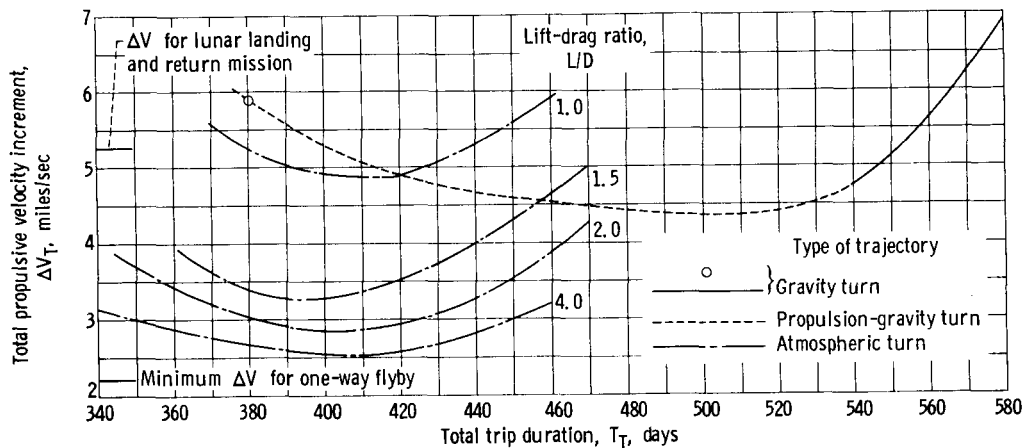


Figure 31. - Mars nonstop round trips, Launch year, 1979 to 1980.

spheric turn trajectories is their comparatively low propulsive ΔV 's.

Comparison of Trajectories

A summary of the propulsive ΔV 's against trip time is shown in figures 30 and 31 for the three types of trajectories evaluated and for the years of 1970 to 1971 and 1979 to 1980. For reference, the total ΔV required for a 6-day lunar round trip based on a direct landing and using atmospheric braking at Earth return, 5.3 miles per second, and the ΔV for a one-way Mars flyby, 2.2 miles per second, are indicated in the figures.

The Mars round trips of interest require values of ΔV substantially less than that for a lunar round trip. The Mars trip times, however, are much longer than the time for the lunar trip, that is, 280 to 580 days compared with 6 to 7 days.

Gravity turn trajectories are possible only at total trip times of approximately 1.0 year and again at trip times that are greater than about 1.5 years. If 1979 to 1980 is the launch year, the lowest ΔV for a gravity turn occurs for a trip time of 540 days.

TABLE IV. - (COMPARISON OF SELECTED NONSTOP ROUND TRIPS

Type of trip	Launch year	Total trip duration, T_T , days	Total propulsive velocity increment, ΔV_T , miles/sec	Velocity arriving at Earth, $V_{p,4}$, miles/sec	Velocity arriving at Mars, $V_{p,2}$, miles/sec	Maximum g-load for maneuver at Mars, G_{max} , Earth g's
Atmospheric turn (lift-drag ratio, 2.0)	1970 to 1971	420	2.85	8.75	6.18	3.0
	1979 to 1980	420	2.95	12.44	7.83	4.8
Propulsion-gravity turn	1970 to 1971	420	3.35	9.73	----	$\sim 10^{-3}$
	1979 to 1980	420	4.9	12.51	----	$\sim 10^{-3}$
Gravity turn	1970 to 1971	365	4.3	9.1	----	----
	1979 to 1980	380	5.9	13.7	----	----
	1970 to 1971	540	3.2	8.9	----	----
	1979 to 1980	540	4.6	11.75	----	----

By admitting the use of thrusting near Mars, the propulsion-gravity-turn type of trajectory becomes possible over a wide range of trip times. For 1979 to 1980, the minimum ΔV is slightly less than that for the best gravity turn and occurs at a shorter trip time, about 500 days. Also, in both 1970 to 1971 and 1979 to 1980, there is only a slow increase in ΔV with decreasing trip time for trip times down to about 400 days.

Even further reductions in ΔV occur when an aerodynamic turn is used at Mars. Values only slightly greater than that for a one-way transfer occur for a vehicle with a lift-drag ratio of 4. Significant reductions in ΔV below that for the propulsion-gravity turn exist also for the more practical lift-drag ratios of 1.5 and 2.0. The trip times for low ΔV are between about 380 and 420 days for this case.

The effect of launch year on the required ΔV may be seen by comparing the values in figures 30 and 31. For the gravity and the propulsion-gravity turns, the values of ΔV are greater in 1979 to 1980 than in 1970 to 1971. This effect is due to the eccentricity of the Mars orbit. The trips in 1970 to 1971 pass Mars when Mars is near its perihelion, as illustrated in figure 1 (p. 2). The trips in 1979 to 1980, however, pass Mars when Mars is near its aphelion. A comparison of the atmospheric turns in 1970 to 1971 and 1979 to 1980 shows that the required propulsive velocity increment for this type of trajectory is least sensitive to the launch year.

Table IV summarizes the remaining mission parameters for selected missions: the 1-year and 540-day gravity turns, the 420-day propulsion-gravity turn, and the 420-day atmospheric turn with an L/D of 2.0. The approach velocities at Earth are comparable for the three mission types. This velocity is highest for the 1-year gravity turn and the propulsion-gravity turn missions in

1979 to 1980. The g-loads required for the maneuver at Mars are the greatest for the aerodynamic turn case but quite modest.

Sketches of the interplanetary trajectories for the 1970 to 1971 minimum ΔV missions of table IV are shown in figure 32. There are several observations to be made about these trajectories:

(1) They all pass Mars (positions 2 and 3) when Mars is near its perihelion.

(2) In general, the outbound leg is a direct trajectory (i.e., it passes through neither an aphelion nor a perihelion), and the return leg is an indirect trajectory (i.e., it passes through both an aphelion and a perihelion). For trips of nearly 1.5 years duration, the outbound leg is a perihelion trajectory. Longer trip times are associated primarily with earlier launch dates, as may be judged from the position of Earth at launch (position 1).

Corresponding to the interplanetary trajectories of figure 32, figures 33 and 34 show the trajectories in the vicinity of Mars approximately to scale and in Mars-centered coordinates. These figures illustrate the view of Mars from the passing vehicle. For all the trajectories, the flight vehicle would approach Mars from ahead of the planet and from below the local horizontal (i.e., the line perpendicular to the radius vector from the Sun, at Mars), and leave Mars above the local horizontal. As already mentioned, the gravity turn trips of longer than 548 days pass Mars on the Sun side, and thus offer a good view of the sunlit side. A 560-day trip is shown in figure 33. The trips that are shorter than 548 days pass on the so-called dark side. The 520-day trip (see fig. 33 also), however, approaches Mars from 40° off the Mars-Sun line and thus offers an oblique view of the sunlit side. The 360-day gravity turn trip offers a similar view.

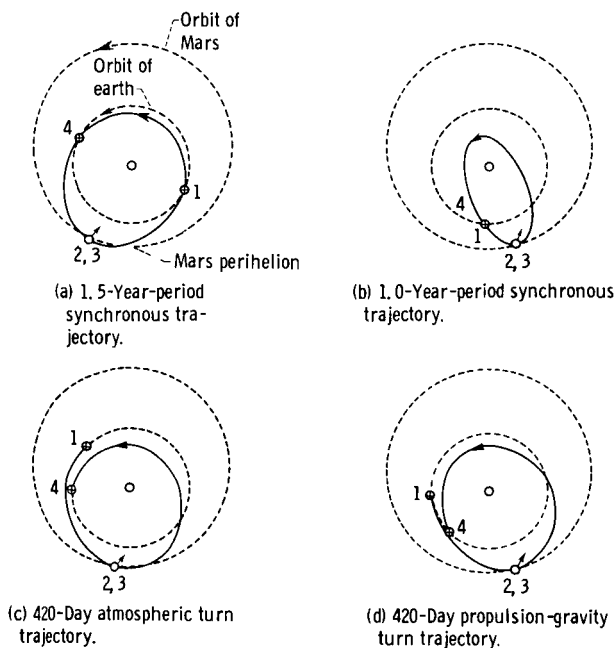


Figure 32. - Mars nonstop round-trip trajectories. Launch year, 1970 to 1971.

The 420-day propulsion-gravity turn trajectory (fig. 34) approaches Mars from 37° off the Mars-Sun line and also yields an oblique view of the sunlit side. The 420-day atmospheric turn trajectories approach Mars from only about 10° off the Mars-Sun line and thus give an almost direct view of the sunlit side. In general, all three types of trajectories can provide at least an oblique view of the sunlit side of Mars.

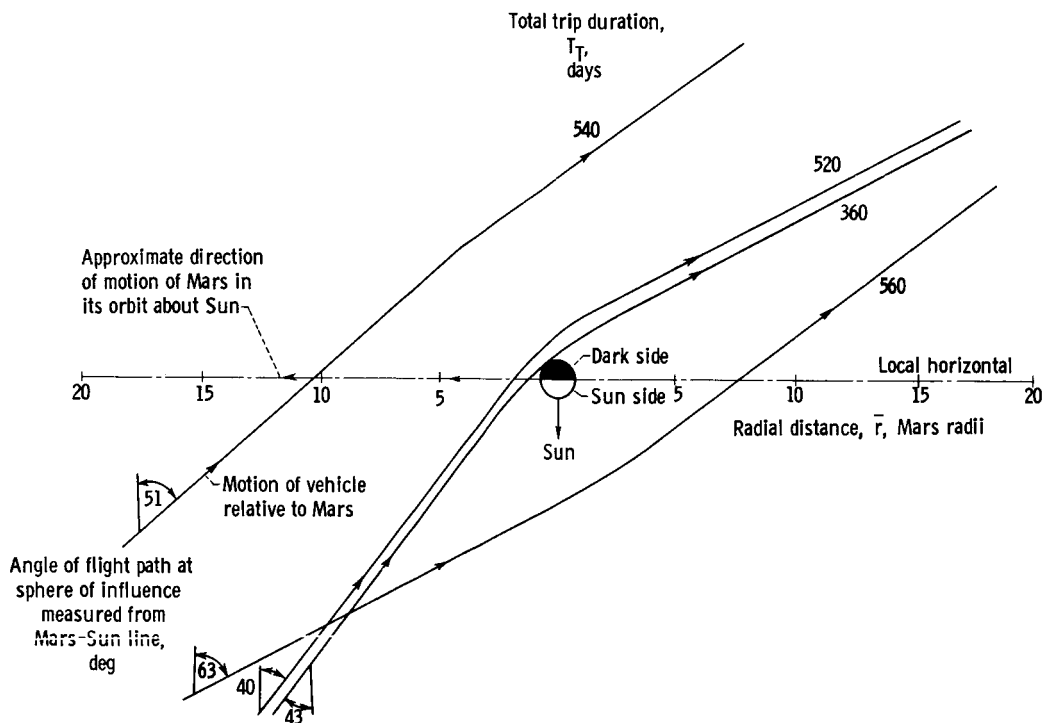


Figure 33. - View of Mars for gravity turn trajectories. Launch year, 1970 to 1971.

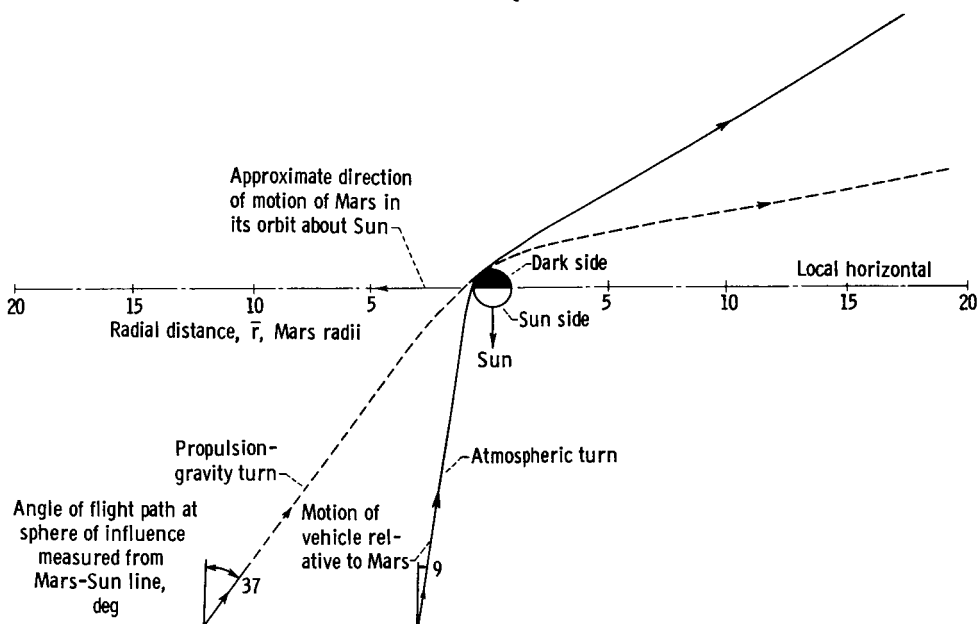


Figure 34. - View of Mars for atmospheric and propulsion-gravity turn trajectories. Launch year, 1970 to 1971; total trip duration, 420 days.

CONCLUSIONS

The following conclusions can be drawn from the present study of Mars non-stop round-trip trajectories using gravity, propulsion-gravity, and atmospheric turns at Mars:

1. When compared with gravity turns, the use of propulsion near Mars markedly expands the range of possible trip times and favorable launch dates and, in some cases, reduces the required total propulsive velocity increment.

2. Atmospheric turn trajectories at Mars can yield the lowest propulsive velocity increments. The values approach that for a one-way flyby of Mars for high vehicle lift-drag ratios. Low propulsive velocity increments occur for trip times down to about 1 year.

3. In general, greater propulsive velocity increments are required in 1979 to 1980 than in 1970 to 1971. The propulsive velocity increments for the atmospheric turn trajectories are the least affected by the launch year.

4. The maximum g-loads associated with the atmospheric turn mission are less than 7 Earth g's for vehicles with a lift-drag ratio of 1.5 or greater.

5. For atmospheric turn and propulsion-gravity turn trajectories with low propulsive velocity increments, the Earth approach velocities are less than twice Earth circular velocity for the 1970 to 1971 launch year, but they increase to about 2.5 Earth circular velocity for 1979 to 1980.

6. For the atmospheric turn trajectories, vehicles with a lift-drag ratio of 1.5 or greater are desirable. The atmospheric entry velocities at Mars for a vehicle with a lift-drag ratio of 1.5 or greater are less than 37,000 feet per second in 1970 to 1971 and less than 47,000 feet per second in 1979 to 1980.

7. All three trajectory types can offer at least an oblique view of the sunlit side of Mars.

8. The propulsion-gravity and atmospheric turn trajectories offer the potential of fast nonstop round trips to Mars with low propulsion requirements. In particular, the possibility of a mission in the early 1970's of about 400 days duration and based on a propulsion-gravity turn or an atmospheric turn trajectory warrants further consideration.

Lewis Research Center

National Aeronautics and Space Administration

Cleveland, Ohio, October 8, 1964

APPENDIX A

SYMBOLS

F	thrust applied at 1.1 Mars radii for propulsion-gravity turn
G_{\max}	maximum force or g-load on vehicle, Earth g's
g	acceleration due to gravity
JD_1	launch date from Earth
L/D	ratio of lift to drag
m	mass of atmospheric turn vehicle
r	radial distance from center of planet to vehicle, miles
\bar{r}	r/r_σ
r_p	periapsis of Mars passage
r_σ	radius of Mars surface
T_O	transfer time from Earth to Mars, days
T_T	total trip duration, days
t	time
ΔV	propulsive velocity increment
V_c	circular velocity at periapsis of planetocentric trajectory, miles/sec
ΔV_G	minimum ΔV for single-impulse transfer between hyperbolic trajectories (from ref. 7)
V_H	heliocentric velocity of spacecraft, miles/sec
V_h	hyperbolic excess velocity of spacecraft (occurs at sphere of influence), miles/sec
ΔV_h	propulsive velocity increment applied at Mars sphere of influence, miles/sec
\bar{V}_h	dimensionless hyperbolic excess velocity, V_h/V_c
V_p	velocity at periapsis of planetocentric trajectory, miles/sec

ΔV_p	characteristic propulsive velocity increment for thrusting at 1.1 Mars radii, miles/sec
\bar{V}_p	dimensionless planet periapsis velocity, V_p/V_c
ΔV_T	total propulsive increment for nonstop missions, miles/sec
ΔV_1	propulsive velocity increment to leave Earth, miles/sec
V_o	velocity of Mars in its orbit, miles/sec
α	angle between vehicle heliocentric velocity vector and local horizontal
β	required flight path turning above that provided by gravity turning
β_A	flight path turning achieved during flight through Mars atmosphere
β_h	flight path turning achieved by thrusting at Mars sphere of influence
β_p	flight path turning achieved during thrusting at 1.1 Mars radii
γ	angle between thrust vector and flight path (local horizontal) for thrusting at 1.1 Mars radii
δ_2	flight path turning due to gravity from arriving sphere of influence to initial periapsis of Mars-centered trajectory
$\delta_{2,3}$	total turning along hyperbolic trajectories from arriving to departing sphere of influence
δ_3	flight path turning due to gravity from final periapsis to departing sphere of influence
ϵ	angle between Mars velocity vector and local horizontal
θ	total required turning angle measured at Mars sphere of influence
μ	gravitational force constant, miles ³ /sec ²

Subscripts:

A	atmospheric turn
c	circular orbit
h	sphere of influence
max	maximum
P	propulsion-gravity turn
p	periapsis

\bar{r}	at \bar{r}
T	total
\oplus	Earth
\circ	Mars
1	departure from Earth
2	arrival at Mars
3	departure from Mars
4	arrival at Earth

APPENDIX B

COMPARISON OF PRESENT AND OPTIMUM TECHNIQUES FOR THRUSTING AT MARS

The present report considers thrusting at essentially two locations, the sphere of influence and the trajectory periapsis, to calculate the ΔV to transfer between two hyperbolic trajectories at Mars. This approach was convenient analytically. The optimum location for transferring between two hyperbolic trajectories by means of a single impulse is analyzed in reference 7. In this appendix, the results of reference 7 are used to indicate the degree of conservatism of the present approach.

The differences in the ΔV for thrusting at the locations assumed in the present analysis and the ΔV for thrusting at the best location $\Delta \bar{V}_G$ are shown in figure 35. The parameter $\Delta \bar{V}_h - \Delta \bar{V}_G$ applies for thrusting at the sphere of influence and $\Delta \bar{V}_p - \Delta \bar{V}_G$ for finite thrusting at trajectory periapsis. Consistent with the analysis of reference 7, the velocities are made dimensionless by dividing by the circular velocity at periapsis, 1.1 Mars radii. A zero value of the parameter indicates zero differences from the optimum. The aforementioned parameters are plotted against the dimensionless approach velocity for two turning angles at the sphere of influence θ and several values of the ratio of hyperbolic leaving to arriving velocity $V_{h,3}/V_{h,2}$. It is assumed here that the transfer takes place on the outbound leg of the approach hyperbola. In figure 35, the solid curves with positive slope apply for thrusting at the periapsis, and the solid and dashed curves

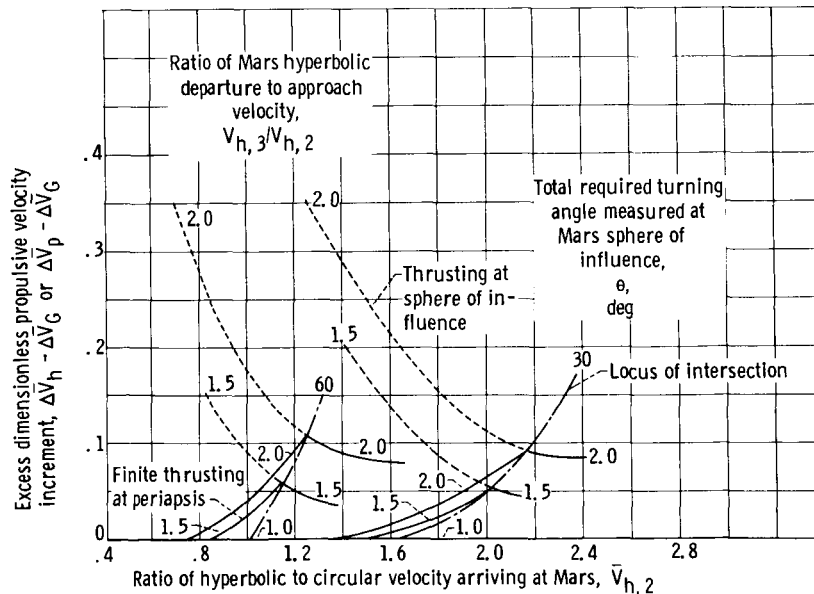


Figure 35. - Comparison of present method of calculating propulsive ΔV at Mars with optimum single impulse ΔV of reference 7. Circular velocity at periapsis of Mars-centered trajectory, 2.14 miles per second.

with negative slope apply for thrusting at the sphere of influence. The dash-dotted lines give the locus of intersections between the two curves. To the left of the intersecting points, thrusting at the periapsis gives the lower ΔV ; to the right of the intersection, thrusting at the sphere of influence is superior. Of course, the lower ΔV is selected in every case. The maximum conservatism occurs along the locus of intersections, decreases as $V_{h,3}/V_{h,2}$ decreases, and approaches zero as $V_{h,3}/V_{h,2}$ goes to 1.0.

For the situation where the optimum location of a single impulse is at the periapsis, the present method of periapsis thrusting (see ANALYSIS) gives values of ΔV equivalent to those of reference 7, that is, $\Delta \bar{V}_p - \Delta \bar{V}_G = 0$. When no velocity change is required (i.e., $V_{h,3}/V_{h,2} = 1.0$) and only turning is required, thrusting at the sphere of influence would be best, that is, $\Delta \bar{V}_p - \Delta \bar{V}_G = 0$. This trend can be seen in the segments of the curve with negative slopes.

The last two columns of table II (p. 18) show the values of θ , $V_{h,3}/V_{h,2}$, and $\bar{V}_{h,2}$ corresponding to the minimum ΔV_T missions that are summarized in figure 14 (p. 17). For trip times of less than 480 days, $V_{h,3}/V_{h,2}$ is less than 1.3 and the turning angles are between 40° and 73° . The conservatism for these cases is estimated from figure 35 to be less than 0.06 mile per second or less than 2 percent of the total ΔV_T shown in figure 14. The conservatism for the 500- and 520-day trips may be somewhat larger than this. At 540 days, however, gravity turns are possible and the thrusting at Mars is eliminated.

For those regions of total trip times where propulsive-gravity turns give lower values of ΔV_T than gravity turns do, it was found that, for 1970 to 1971, thrusting at the departing sphere of influence was the best of the alternative locations considered. This was also true for 1979 to 1980 for trip times of less than 500 days. For trip times of about 500 to 540 days in 1979 to 1980, lower values of ΔV_T result for thrusting at periapsis.

Thus, the best of the present alternatives for thrusting at Mars results, at worst, in a total mission ΔV that is only slightly higher (2 percent) than would be found if optimum single impulse thrusting were used.

REFERENCES

1. Ross, Stanley: A Systematic Approach to the Study of Nonstop Interplanetary Round Trips. Vol. 13 of Advances in the Astronautical Sci., E. Burgess, ed., Western Periodicals Co., 1963, pp. 104-164.
2. Knip, Gerald, Jr., and Zola, Charles L.: Three-Dimensional Sphere-of-Influence Analysis of Interplanetary Trajectories to Mars. NASA TN D-1199, 1962.
3. Ross, Stanley, et al.: Space Flight Handbooks, vol. 3: Planetary Flight Handbook, pts. 1, 2, and 3. NASA SP-35, 1963.
4. Ehricke, Krafft A.: Space Flight. I. Environment and Celestial Mechanics. D. VanNostrand Co., Inc., 1960.
5. Luidens, Roger W.: Flight-Path Characteristics for Decelerating from Supercircular Speed. NASA TN D-1091, 1961, p. 11.
6. McLaughlin, John F.: Sizing Nuclear Orbital Launch Vehicles for Interplanetary Missions. Astronautics and Aeronautics, vol. 2, no. 2, Feb. 1964, pp. 70-76.
7. Gobetz, Frank W.: Optimum Transfers Between Hyperbolic Asymptotes. AIAA Jour., vol. 1, no. 9, Sept. 1963, pp. 2034-2041.
8. Fimple, W. R.: Optimum Midcourse Plane Changes for Ballistic Interplanetary Trajectories. AIAA Jour., vol. 1, no. 2, Feb. 1963, pp. 430-434.
9. Goebel, T. P., Martin, J. J., and Boyd, J. A.: Factors Affecting Lift-Drag Ratios at Mach Numbers from 5 to 20. AIAA Jour., vol. 1, no. 3, Mar. 1963, pp. 640-650.
10. Seifert, Howard S., ed.: Space Technology. John Wiley & Sons, Inc., 1959.
11. Seiff, Alvin: Atmosphere Energy Problems of Manned Interplanetary Flight. Proc. AIAA and NASA Conf. on Eng. Problems of Manned Interplanetary Exploration, Palo Alto, Calif., Sept. 30-Oct. 1, 1963, pp. 19-33.